Doctoral Dissertation

Unique Morphology of Poly(lactic acid) Monoliths

via Thermally Induced Phase Separation

熱誘起相分離法を介するポリ乳酸モノリスの特異構造

Tomonari Kanno

January 2018

Graduate School of Engineering,

Osaka University

Contents

General introduction

Currently, environmental issues have been discussed all over the world. The major concerns we face may include global warming, resource depletion, ozone layer depletion, deforestation, waste disposal, and overpopulation, which have been arisen from harmful effects of human activities on the environment. Among these problems, global warming can be the greatest threat we have ever faced, that requires immediate attention.

Global warming is believed to be primarily caused by increases in greenhouse gases such as carbon dioxide (CO_2), methane (CH_4), Nitrous oxide (N_2O), hydrofluorocarbons (HFCs), perfluorocarbons (PFCs), and sulfur hexafluoride (SF6) resulting from human activities. Especially, CO_2 has been considered as the most influential factor to the increase in average global temperature due to its considerable amount of emission and greenhouse effect, for which the measures to limit the release of CO_2 have been discussed at a nation level. In Japan, the Kyoto Protocol was adapted, setting a target for at least 6% reduction of greenhouse gases compared with that in 1990 during four years between 2008 and 2012. More recently, in 2013, 3.8% reduction of these gases compared to 2005 was settled as a new goal before 2020.

One of the major factors of the increase in CO_2 emission can be excessive dependence on petroleum oil among human activities because combustion of the oil can lead to one-way CO_2 release to the atmosphere. However, it was reported that the rate of dependence on petroleum oil within the country reached to more than 40% in 2013.[1] Therefore, the reduction in CO_2 emission may not be achieved without breakaway from dependence on petroleum resources.

One of the most dependent materials on petroleum oil for production is a

plastic. Currently, more than 11 million tons of plastics are consumed in Japan every year, and most of these are petroleum-derived products such as polyethylene (PE), polypropylene (PP), polystyrene (PS), poly(vinyl chloride) (PVC), and phenolic resins. These plastics are synthesized from finite petroleum resources, emitting considerable amount of CO_2 to the atmosphere during its production and combustion processes. In addition, since these oil-based plastics are generally not degradable to the environment, negative effects to ecosystem such as pollution on the sea and accidental ingestion by animals are concerned all over the world.[2] In contrast, compared with these petrochemical products, eco-friendly plastics with growing demand are bio-plastics.

Bio-plastics can be divided into two categories: biodegradable plastics and biomass plastics. Biodegradable plastics are defined as resins that are degraded to CO_2 and water by the action of microorganisms in soil and water. In contrast, biomass plastics are defined as materials synthesized from renewable natural resources without fossil resources, which is expected to reduce house-effect gases.[3] Figure 1 summarizes recent major biodegradable and biomass polymers.

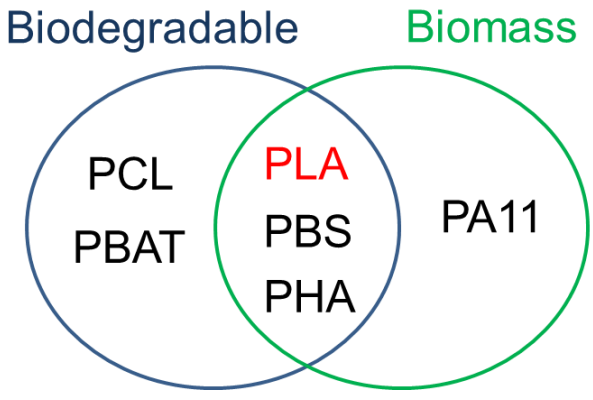

Figure 1. Classification of bio-plastics [PLA: poly(lactic acid), PBS: poly(butylene succinate), PHA: poly(3-hydroxyalkanoate), PCL: poly(ε-caprolactone), PBAT: poly(butylene adipate-co-butylene terephthalate). PA11: polyamide 11].

In the group of bio-plastic, there are biomass polymers such as poly(lactic acid) (PLA), poly(butylene succinate) (PBS), and poly(3-hydroxyalkanoate) (PHA) that exhibit biodegradability simultaneously. Among these plastics, particularly, the material with high physical properties, producibility, environmental adaptability, and huge demand is poly(lactic acid).

Poly(lactic acid) is a 100% bio-based polymer with great biodegradability and biocompatibility, which derived from renewable resources such as agricultural products and their by-products including a stem and a leaf (Figure 2). Because of its environmental adaptability, PLA has received great attention to the development of a sustainable society. PLA can be finally degraded to CO_2 and water in the environment, and the resultant products are recycled as carbon resources for plants to produce new PLA. Thus, PLA shows carbon neutrality, preventing one-way increase of CO_2 to the atmosphere when its production and combustion process (Figure 3). In addition to its great biodegradability and biocompatibility, PLA has remarkable processability due to its higher glass transition (*ca*. 60 ^{o}C) and melting temperature (*ca*. 170 ^{o}C) compared to other bio-based plastics.[4] Moreover, PLA exhibits sufficient mechanical strength and high transparency comparable to oil-based polymers such as poly(ethylene terephthalate) (PET), polypropylene (PP) (Table 1).[2] Besides, PLA can be degraded by catalyst-free simple hydrolysis without toxic degradation products, for which PLA is approved by the US Food and Drug Administration (FDA) for several medical uses.[5,6]

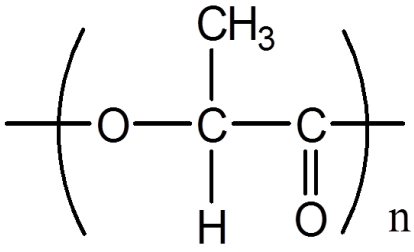

Figure 2. Chemical structure of PLA.

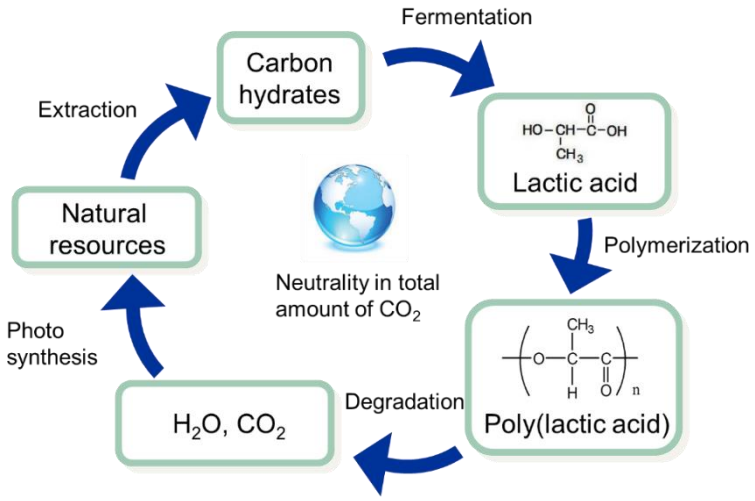

Figure 3. Carbon neutrality of PLA.

Table 1. General properties of bio-based polymers and oil-based polymers.

	Bio-based polymer			Oil-based polymer	
	PLA	PBS	PHA	PET	PP
T_g (°C)	58-60	-32	-60	80	5
T_m (°C)	160-170	114	60	260	164
Tensile strength (MPa)	68	57	61	57	32

PLA: poly(lactic acid), PBS: poly(butylenes succinate), PHA: poly(3-hydroxyalkanoate), PET: poly(ethylene terephthalate), PP: polypropylene.

Thanks to these unique properties and great developments in industrialization of PLA over decades, the use of PLA materials has been spread to various fields including medical, foods, packaging, and even housewares in a different form with increasing awareness to environmental conservation.[2] For example, PLA was used as biodegradable food trays in a restaurant in world Expo 2005 (Exposition of Global Harmony), which inspired us new generation of bio-plastics. In addition, the automobile named "SAI" was launched in 2009 from Toyota Motor Corporation, wherein PLA materials were utilized as interior and exterior car parts. Thus, PLA has been attempted

to apply in tremendous fields not only as alternatives of oil-based polymers but also as new functionalized materials taking advantage of PLA. Expanding and finding a new application of PLA can increase in use of PLA and lead breakaway from petroleum society.

Monolithic porous PLA has also been developed in several fields such as tissue engineering, drug delivering, and filtration technology with recent technical innovation in human iPS cells and seawater desalination concerning worldwide water shortage. In general, monoliths are functional materials with a 3D continuous framework in a single piece.[7] Due to its 3D structure and high surface area, monoliths exhibit fast mass transfer of reagent solution and usefulness as a medium culture, for which monoliths has been fascinating materials to a number of fields. Since the monolith form of PLA has great advantages in surface area, light weight, and 3D framework in addition to the environmental adaptability, the use of PLA monolith has been expanded to a scaffold for cultivating human cell,[8] an artificial bone,[6,9,10] a support for controlled release of drugs,[5,11] and a filter.[12-14] For instance, Tanaka *et al*. reported PLA monoliths which can be used as filters for seawater desalination.[12-14] These PLA filters are expected to contribute to waste reduction since it can be compostable after clogging.

The monolith formation has been developed using a variety of methods including porogen, fiber bonding, gas-based foaming, a use of supercritical CO_2, and 3D printing.[5,8,15-17] However, these methods have critical drawbacks such as formation of discontinuous pores, complicated procedures, high-cost, and low reproducibility, which limit controllability in morphology of PLA monoliths. Especially, for the usage mentioned above, it is important to synthesize monoliths through the process with precise controllability in morphology and reproducibility because the function of

monoliths such as biodegradation rate, hydrophobicity, and adhesiveness significantly depends on its pore and skeletal size. Therefore, exploring a method with process flexibility has been attempted to prepare desirable formation suitable for each usage.

Among these techniques of producing PLA monoliths, recently, phase separation has been utilized due to its excellent versatility, simplicity, and controllability in pore size compared to other methods.[12-14,18-23] Furthermore, good processability is also key factor of this method since the shape of monolith is dependent on the shape of vessels where the phase separation and gelation take place. This method can mainly be classified into two for preparation of PLA monoliths by the types of trigger to occur phase separation: non-solvent induced phase separation (NIPS) and thermally induced phase separation (TIPS). Table 2 summarizes the representative examples of PLA monoliths and their procedure.

Table 2. Representative PLA monoliths produced *via* phase separation method.

Purpose	Method	Solvent (good/poor)
artificial bones[18]	NIPS	dichloromethane/hexane
hydrophobic surface[19]	NIPS	*N*-Methyl-2-pyrrolidone/water
filters[20]	NIPS	*N*-Methyl-2-pyrrolidone/water
filters[12]	TIPS	1,4-dioxane/water
rigid form[21]	TIPS	tetrahydrofuran/water
case study[22]	TIPS	1,4-dioxane/water

These techniques were previously explained in detail by Lloyd *et al*. using the Flory-Huggins theory.[24,25] Briefly, the change in polymer fraction in a ternary system of

polymer, good solvent, and non-solvent increases Gibbs free energy which triggers phase separation. Until the mixing of polymer-lean and polymer-rich phases becomes stable, phase separation continues to satisfy the lowest Gibbs free energy. At this process, the system undergoes liquid-liquid and/or solid-liquid phase separation depending on the composition and temperature, which determines the final morphology of monoliths. It is well known that liquid-liquid phase separation gives interpenetrating 3-D network *via* spinodal decomposition, whereas solid-liquid phase separation leads to the sea-island morphology including polymer precipitation *via* nucleation and growth mechanism.[25]

In the NIPS method, addition of non-solvent to polymer solution induces phase separation.[24,25] This method has been traditionally utilized for fabricating filtration membranes. The morphology of obtained monoliths can be changed by various factors such as selection of solvent and polymer, solvent ratios, polymer concentration, molecular weight, and standing temperature. Few researchers attempted to produce PLA monoliths by NIPS.[18-20] For example, Rezabeigi *et al*. produced PLA monoliths by NIPS using dichloromethane (DCM) as a polymer solvent and hexane as a non-solvent.[18] They reported that PLA monoliths with the porosity ranging from 40.7% to 90.7% and meso/macroporous hierarchical morphology were successfully fabricated by changing the DCM ratio and the PLA concentration during phase separation.

By contrast, TIPS method has also been utilized to prepare PLA monolith.[12-14,20-23] In the TIPS method, the drop in polymer solubility induced by solution temperature leads phase separation. Distinct from NIPS process, TIPS has remarkable advantages in reproducibility and flexibility since the phase separation is occurred by simple temperature reduction rather than non-solvent exchange including

variables that need to be controlled.[24] Furthermore, the morphology can be controlled by changing quench temperature in addition to those controlling factors of NIPS as mentioned. In addition, TIPS process is applicable to a wide range of materials including semi-crystalline polymers with no soluble solvent at room temperature.[24] Because of these merits, a number of monoliths were previously synthesized *via* TIPS technique from versatile petroleum plastics such as polyolefin,[26,27] polymethylmethacrylate (PMMA),[28,29] and PS.[30] In general, binary good/poor solvent is used to induce phase separation and gelation through solubility gap during quenching. Önder *et al*. successfully produced PLA monoliths with high porosity ranging from 85.1 to 92.8% through TIPS method using tetrahydrofuran (THF) as a good solvent and water as a non-solvent. They reported that the pore size of PLA monoliths can be manipulated in a range of 25-400 μm by changing solvent ratio, polymer concentration, and quenching temperature.[21] Thus, utilization of TIPS can be ideal for producing PLA monoliths with good controllability in morphology due to its high reproducibility and simplicity, which significantly contributes to the applications mentioned above.

Even though various PLA monoliths have been fabricated *via* TIPS, unfortunately, the use of the monolith is still limited due to its micron scale morphology. Moreover, several physical properties of PLA monoliths are insufficient for use mentioned above. For instance, its low thermal properties and chemical resistance are critical disadvantages for medical use.[31] In addition, notably high hydrophobic surface of the monoliths limits applications especially in scaffolds and filters.[32] Therefore, it is desired to produce reinforced PLA monoliths suitable for each application, which can open the use of PLA monoliths and contribute to the sustainable society.

This doctoral thesis reports the functionalization of PLA monoliths *via* TIPS using novel strategy. This thesis contains 3 chapters.

Contents of this thesis

Chapter 1

Poly(L-lactic acid) (PLLA) monolith with micron to nano scale of pore and skeletal size was fabricated *via* novel TIPS method using ternary solvent, elucidating the relationships between structures and characteristics through phase diagram in the system and thermo-analysis. TIPS was conducted using combination of good solvent, non-solvent, and mid-solvent which controls phase separation. The effect of mid-solvent on morphology and crystallization of PLLA was studied. In addition, pore and skeletal size of PLLA monoliths were controlled by changing parameters in the system. TIPS with precise controllability in morphology has huge advantage to the usage of PLLA monoliths such as a scaffold, an artificial bone, a support for drugs, and a filter.

Chapter 2

PLA monoliths containing stereocomplex (sc) crystals were produced from enantiometric PLLA and poly(D-lactic acid) (PDLA) *via* TIPS developed in Chapter 1. The monoliths were prepared with changing the ratio of PLLA/PDLA during phase separation process. The influence of the addition of PDLA on morphology was studied focusing on crystallization behavior. Furthermore, the change in thermal properties and chemical resistance were observed comparing with pristine PLLA monoliths. The present PLLA/PDLA monoliths with reinforced physical properties have great potential for usage in medical fields.

Chapter 3

A new method was developed for producing monolithic composites of PLLA and bacterial cellulose (BC) gel through both TIPS developed in Chapter 1 and freeze-drying technique. BC/PLLA monoliths exhibited unique double network wherein PLLA unit and BC fiber were co-existed. The effect of interpenetrated BC was investigated to reveal the change in both mechanical properties and hydrophilicity of the monoliths. The proposed method allows PLA monoliths to have desirable physical properties, which can significantly expand the use of PLLA monoliths especially in water environment.

References

1. Agency for Natural Resources and Energy In *Japan's Energy White Paper 2016* Japan, **2016**.
2. Oshima, K. In Technology and Market Development of Green Plastic Polylactide (PLA), Eds,; Frontier Publishing Co., Ltd: Japan, **2005**; p 3-12.
3. Iwata, T. *Angew. Chem. Int. Ed*. **2015**, 54, 3210-3215.
4. Ikada, Y.; Tsuji, H. *Macromol. Rapid Commun.* **2000**, 21, 117-132.
5. Jacobson, G. B.; Shinde, R.; Contag, C. H.; Zare, R. N. *Angew. Chem. Int. Ed.* **2008**, 47, 7880-7882.
6. Rezabeigi, E.; Wood-Adams, P. M.; Drew, R. A. L. *Polymer* **2014**, 55, 3100-3106.
7. Svec, F.; Fréchet, J. M. *Anal. Chem.* **1992**, 64, 820-822.
8. Liu, C.; Wong, H. M.; Yeung, K. W. K.; Tjong, S. C. *Polymers* **2016**, 8, 287-306.
9. Rezwan, K.; Chen, Q. Z.; Blaker, J. J.; Boccaccini, A. R. *Biomaterials* **2006**, 27, 3413-3431.
10. Obata, A.; Ozasa, H.; Kasuga, T.; Jones, U. R. *J. Mater. Sci.: Mater. Med.* **2013**, 24, 1649-1658.
11. Tyler, B.; Gullotti, D.; Mangraviti, A.; Utsuki, T.; Brem, H. *Adv. Drug. Deliv. Rev.* **2016**, 107, 163-175.
12. Tanaka, T.; Lloyd, D. R. *J. Membr. Sci.* **2004**, 238, 65-73.
13. Tanaka, T.; Eguchi, S.; Aoki, T.; Tamura, T.; Saitoh, H. Taniguchi, M. Ohara, H.; Nakanishi, K.; Lloyd, D. R. *Biochem. Eng. J.* **2007**, 33, 188-191.
14. Tanaka, T.; Nishimoto, T.; Tsukamoto, K.; Yoshida, M.; Kouya, T.; Taniguchi, M.; Lloyd, D. R. *J. Membr. Sci*. **2012**, 396, 101-109.
15. Mikos, A. G.; Thorsen, A. J.; Czerwonka, L. A.; Bao, Y.; Langer, R.; Winslow, D.

N.; Vacanti, J. P. *Polymer* **1994**, 35, 1068-1077.

16. Nofar, M.; Park, C. B. *Prog. Polym. Sci.* **2014**, 39, 1721-1741.
17. Serra, T.; Planell, J. A.; Navarro, M. *Polymer* **2013**, 9, 5521-5530.
18. Rezabeigi, E.; Wood-Adams, P. M.; Drew, R. A. L. *Polymer* **2014**, 55, 6743-6753.
19. Gao, A.; Zhao, Y.; Yang, Q.; Fu, Y.; Xue, L. *J. Mater. Chem. A.* **2016**, 4, 12058-12064.
20. Domingues, R. C. C.; Pereira, C. C.; Borges, C. P. *Macromol. Symp.* **2016**, 368, 128–135.
21. Önder, Ö. C.; Yilgöl, E.; Yilgöl, I. *Polymer* **2016**, 107, 240-248.
22. Mannella, G. A.; Pavia, F. C.; Carrubba, V. L.; Brucato, V. *Eur. Polym. J.* **2016**, 79, 176-186.
23. Nie, T.; He, M.; Ge, M.; Xu, J.; Ma, H. *Appl. Polym. Sci.* **2017**, 134, 44885-44895.
24. Lloyd, D. R. Kim, S. S.; Kinzer, K. E. *J. Membr. Sci.* **1991**, 64, 1-11.
25. Lloyd, D. R.; Kinzer, K. E.; Tsung, H. S. *J. Membr. Sci.* **1990**, 52, 239-261.
26. Kim, J. J.; Hwang, J. R.; Kim, U. Y.; Kim, S. S. *J. Membr. Sci.* **1995**, 108, 25-36.
27. Chung, T. C.; Lee, S. H. *J. Appl. Polym. Sci*. **1997**, 64, 567-575.
28. Graham, P. D.; Pervan, A. J.; McHugh, A. J. *Macromolecules* **1997**, 30, 1651-1655.
29. Tsai, F. J.; Torkelson, J. M. *Macromolecules* **1990**, 23, 775-784.
30. Kim, S. S.; Lloyd, D. R. *J. Membr. Sci.* **1991**, 64, 13-29.
31. Isama, K. In Bio materials and medical devices - Approach to the safety and Bio compatibility, Eds.; CMC Publishing Co., Ltd: Japan, **2003**; p 25.
32. Ghalia, M. A.; Dahman, Y. *J. Polym. Res*. **2017**, 24, 74.

Chapter 1.

Morphological control of poly(lactic acid) monoliths through novel phase separation technology

1.1 Introduction

As described in general introduction, PLLA monolith with high surface area, light weight, and 3D framework has been developed with increasing importance in several fields such as tissue engineering, drug delivering, and filtration technology. Among methods to produce PLA monoliths, TIPS has been received much attention as a low-cost and low-energy technique due to its high reproducibility, and simplicity.

Despite these fascinating advantages for using TIPS, the precise control to give desirable morphology of PLA monoliths *via* TIPS is still challenge. For instance, Tanaka *et al*. applied this method and reported that PLA monoliths for filtration could be prepared by the TIPS using 1.4-dioxane as a solvent and water as a non-solvent,[1] however, the resultant PLA monoliths mainly exhibited pores in the short range of 10-30 μm with micron scale of frameworks. In contrast, Önder *et al*. developed this idea and reported that PLA monoliths with high porosity ranging from 85.1 to 92.8% and 25-400 μm of relatively large pores were fabricated using tetrahydrofuran (THF) and water solvent system by changing polymer concentration, solvent ratio, and quenching temperature.[2] Although they conducted to control the morphology with various ways, the pore and skeletal size of PLA monoliths were still limited in the micron scale.

In this chapter, it was focused on the production of PLA monolith with micron to nano scale of pore and skeletal size *via* novel TIPS method using ternary solvent, elucidating the relationships between structures and characteristics *via* phase diagram in the system and thermo-analysis. Distinct from the traditional TIPS using binary solvent, the author selected ternary solvents: 1,4-dioxane as a good solvent, water as a non-solvent, and 2-butanone as a mid-solvent which controls phase separation. 2-Butanone was chosen since it exhibits good affinity but no solubility to PLA itself in addition to miscibility with 1,4-dioxane/water. The author demonstrates that the PLA monoliths with unique morphology and precise controllability in pore and skeletal size can be fabricated by amazingly simple, newly developed TIPS.

1.2 Experimental

Materials

PLLA was purchased from NatureWorks LLC (Ingeo^{TM} Biopolymer 4032D, M_w = 1.5 x 10^5 g/mol). 1,4-Dioxane, 2-butanone, and 2-propanol (iPA) were obtained from Nacalai tesque and were used as received.

Ternary phase diagram

For understanding detailed behaviors on phase separation, The author prepared ternary phase diagram of 1,4-dioxane/2-butanone/water at fixed PLLA concentration and temperature by changing the ratio of solvents to give a cloud point of the solution.

First, PLLA was dissolved in 1,4-dioxane/2-butanone mixture at 70 ^oC with the PLLA concentration of 100 mg/mL for 2 h in a glass test jaw. After dissolution, water was added to the solution and then the transparent solution was kept at 70 ^oC or 0 ^oC for 30 min. The cloud point in the system at 70 ^oC and 0 ^oC was defined at which the

solution turned opaque during 30 min. By plotting these cloud points, the borders separated homogenous and heterogenous area at 70 ^{o}C and 0 ^{o}C in the system were determined.

Preparation of PLLA monoliths

At first, PLLA was dissolved in 1,4-dioxane/2-butanone mixture at 70 ^{o}C with the PLLA concentration of 100 mg/mL for 2 h in a glass test jaw. Then, water was added to the solution and stirred for 10 min to give transparent solution. The ratios of ternary solvent were selected from homogenous region surrounded by the boundaries at 70 ^{o}C and 0 ^{o}C in the ternary phase diagram, that is, wherein the homogenous solution at 70 ^{o}C can be phase-separated by quenching to 0 ^{o}C. The solution was immediately cooled to 0 ^{o}C using ice bath for 1 h to induce phase separation. The resultant gels were exchanged to iPA by washing using a TAITEC BioShaker M-BR-022UP at 25 ^{o}C. The obtained gels were placed in a vacuum and dried at room temperature for 5 h to give PLLA dry-monolith. Figure 1-1 shows the sample at each process in this study.

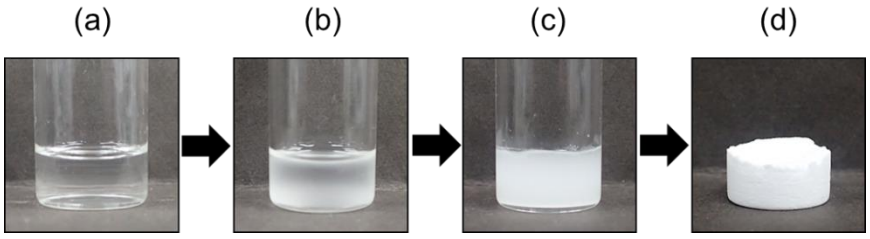

Figure 1-1. Fabrication process of PLLA monoliths in this study: PLLA solution (a), solution undergone phase separation (b), wet gel resulted from gelation (c), PLLA monolith after drying (d).

Additionally, to investigate the influence of PLLA concentration on the formation of PLLA monoliths in the system, extra monoliths were prepared using the same technique mentioned above at fixed (15/80/5) 1,4-dioxane/2-butanone/water ratio with different PLLA concentrations (50-150 mg/mL).

Analysis

Morphology of PLLA monoliths were observed by scanning electron microscopic (SEM) analysis using a HITACHI SU-3500 instrument. Averaged pore diameter was determined using Image-Pro PLUS (MediaCybernetics) by calculating to 50 pores exhibited in the SEM image of the monoliths. Melting temperature (T_m), and crystallinity (X_c) of the PLLA monoliths and the pellet used were estimated by differential scanning calorimetry (DSC) using SEIKO DSC6220, at a heating rate of 10 ^oC/min in a range between 30 and 200 ^oC and a nitrogen flow rate of 50 mL/min. The crystallinity of the PLLA crystals were calculated using the theoretical heat of fusion (93.1 J/g).[3] During the DSC measurements, no peaks ascribable to cold crystallization appeared so that the X_c could be simply estimated from the enthalpy of melting. Porosity of the monoliths was calculated using an apparent density of the monoliths and Eq. (1) given below.[3,4]

$$Porosity\ (\%) = \left(1 - \frac{\rho}{\rho_0}\right) \times 100 \qquad \ldots (1)$$

Here, ρ/ρ_0 represents the relative density where ρ and ρ_0 are respectively the apparent density and skeletal density which can be estimated from Eq. (2)

$$\rho_0 = w_c(\rho_c - \rho_a) + \rho_a \qquad \ldots (2)$$

In the Eq. (2), where w_c represents the crystalline volume ratio, ρ_c is the density of 100% crystalline PLLA (1.290 g/cm^3), and ρ_a is the density of fully amorphous PLLA (1.248 g/cm^3).[3-5] Thus, the ρ_0 can be estimated by measuring the crystallinity of the PLLA monoliths using DSC.

1.3 Results and discussion

Ternary phase diagram

Figure 1-2 gives the ternary phase diagram of 1,4-dioxane/2-butanone/water at PLLA concentration of 100 mg/mL.

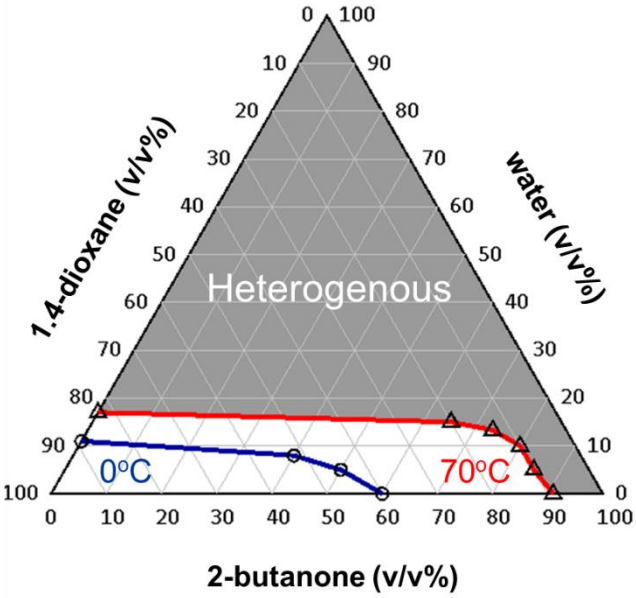

Figure 1-2. Ternary phase diagram of 1,4-dioxane/2-butanone/water system with the fixed PLLA concentration at 100 mg/mL. Note that (△) and (○) symbols represent respectively the cloud point in the system at 70 ^{o}C and 0 ^{o}C. The boundaries separated homogenous and heterogenous (area in grey) regions at 70 ^{o}C and 0 ^{o}C in the system are given in red and blue lines, respectively.

As shown from the diagram, the PLLA solution become heterogenous over 91 v/v% of 2-butanone and 17 v/v% of water contents at 70 ^{o}C, whereas those of maximum contents at 0 ^{o}C are decreased to 60, 11 v/v%, respectively. In this regard, phase separation takes place by quenching from 70 ^{o}C to 0 ^{o}C using the solvent ratio selected from the region surrounded by homo/heterogenous boundaries at 70 ^{o}C and 0 ^{o}C. It is noteworthy that the region between boundaries at 70 ^{o}C and 0 ^{o}C become significantly wider with increasing the ratio of 2-butanone, whereas that in the binary

1,4-dioxane/water system is limited in narrow range between 89/11-83/17 v/v%. These data indicate that PLLA is much more miscible in the ternary 1,4-dioxane/2-butanone/water solvent than the traditional binary 1,4-diaoxane/water solvent, suggesting the slower phase separation can be occurred in the solution with higher 2-butanone content. This effect of phase separation will be discussed in detail later.

Furthermore, this study demonstrates that the addition of mid-solvent may expand selection of controlling factor for pore and skeletal size. For over decades, TIPS with binary good/poor solvent have been widely used,[1,2,6-9] while this often limits the condition of fabrication. For example, Tanaka *et al*. reported that PLLA monoliths were produced by TIPS using binary 1,4-dioxane/water solvent with the limited ratio around 87/13 w/w% at 10 wt% of PLLA concentration.[1] In addition, Önder *et al*. reported PLLA monoliths were successfully fabricated using binary THF/water solvent, however, only narrow range of the THF/water ratio between 90/10-84/16 w/w% can be utilized to give the monolith formation.[2] Therefore, the TIPS using ternary solvent in this study may open the limitation in choice of solvent to add a desirable morphology to monoliths.

Characterization of PLLA monoliths

PLLA monoliths with no visible shrinkage after drying were successfully produced from fully gelated PLLA gels synthesized at the all solvent ratios used which is determined by the ternary diagram. The resultant samples were analyzed by DSC to estimate PLLA crystallinity and porosity of the monoliths, focusing on the influence of the solvent ratio.

In Table 1-1 and Figure 1-3 showing the DSC results, all PLLA monoliths

indicated the T_m peak originated from PLLA crystals at *ca.* 168 °C, which corresponded to 45-67% of high crystallinity.

Table 1-1. Physical properties of PLLA monoliths prepared at different 1,4-dioxane/2-butanone/water ratios.

Systems[a]	T_m [b] (°C)	X_c [c] (%)	Apparent density (g/cm^3)	Porosity[d] (%)
85/0/15	168	45	0.12	90
65/20/15	168	55	0.12	91
45/40/15	169	57	0.11	92
25/60/15	170	59	0.10	92
15/80/5	169	67	0.10	93

a : System corresponds to the solvent ratio of 1,4-dioxane/2-butanone/water (v/v%).

b : T_m = melting temperature of PLLA crystal.

c : X_c = crystallinity of PLLA crystal calculated from DSC measurements assuming the theoretical heat of fusion = 93.1 J/g.[3]

d : Porosity calculated from Eq. (1) and (2) using the apparent density and crystalinity of PLLA monoliths.

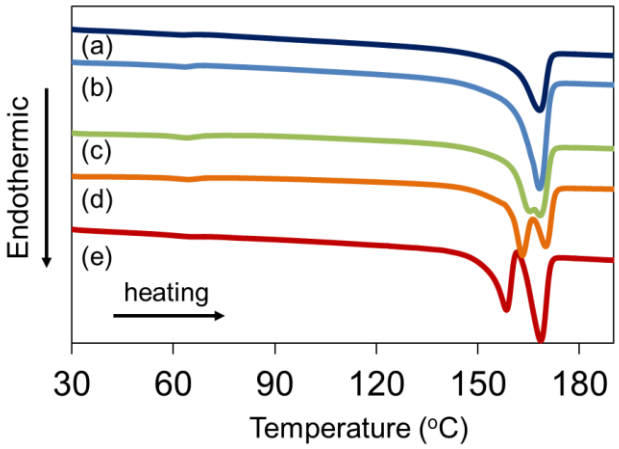

Figure 1-3. DSC thermograms of PLLA monoliths prepared at different 1,4-dioxane/2-butanone/water ratios [(a): 85/0/15, (b):65/20/15, (c):45/40/15, (d):25/60/15, (e): 15/80/5].

Note that the crystallinity become higher with increasing the ratio of 2-butanone which was used in the TIPS process. This can be explained by the difference in speed of phase separation, which is previously discussed in detail by several researchers.[2,5] During quenching process, the phase separation and the gelation caused by crystallization of PLLA are occurred competitively. The crystallization takes place in the polymer rich phase during liquid-liquid phase separation, wherein the solvent diffuses from the polymer-rich phase to lean phase giving the mobility of polymer chain. Namely, the lower phase separation rate is, the slower solvent transport from the polymer-rich phase takes place, which provides sufficient time to form more crystals. Therefore, the speed of phase separation in the system significantly affects on the final morphology and crystallinity of the resultant PLLA monoliths. In this study, as the 2-butanone ratio in the mixture increases, the slower phase separation can be occurred providing more time to facilitate PLLA crystallization during quenching because of its higher miscibility of PLLA than that mixture including larger amount of water (see Figure 1-2). It is also interesting to note that all PLLA monoliths exhibited much higher crystallinity than original PLLA pellet (X_c = 39%) used for preparing the monoliths. This tendency has been also reported previously when using other choices of polymer,[10] however, the mechanism of the crystallization during phase separation has not been fully investigated until now. In the present study, a possible cause of the higher PLLA crystallinity may be induced by the ordering and/or stretching of the polymer chain during phase separation, promoting the formation of PLLA crystallization.

From the estimated PLLA crystallinity, the porosity of all monoliths were successfully calculated from the Eq. (1) and (2) using the apparent density (Table 1-1). These calculations demonstrated that the PLLA monoliths have more than 90% of high

porosity, and was increased from 90 to 93% with higher 2-butanone content. The increase in porosity may due to the shrinkage at gelation process for the system including larger amount of water. During gelation, water can exist on the hydrophilic surface of the glass test container, which can lead to the shrinkage preventing the gel formation at the edge of glass.

Thus, it was revealed that the PLLA monoliths with the high crystallinity and porosity were successfully fabricated through the controlled phase separation using 2-butanone.

Morphology control of PLLA monoliths

Structural analysis was carried out to observe the morphology of PLLA monoliths (Figure 1-4, 1-5).

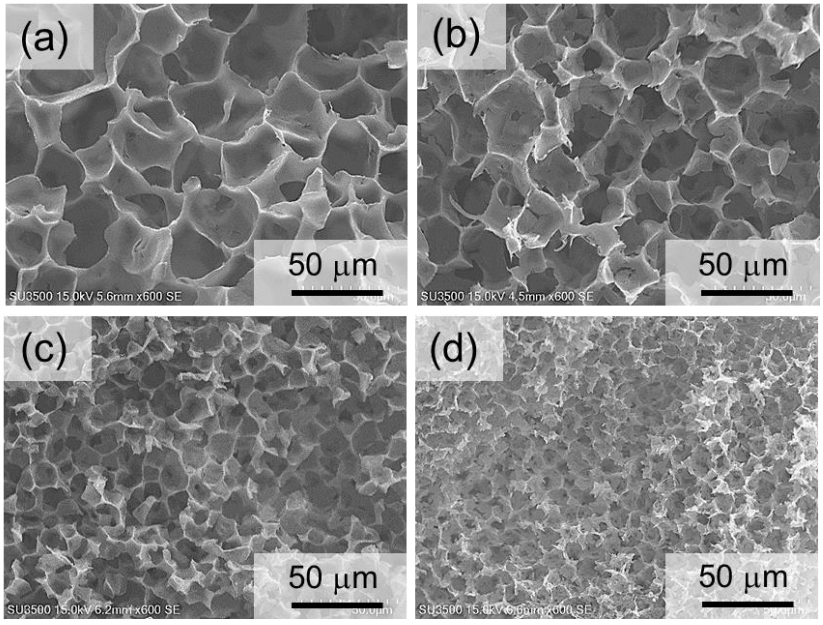

Figure 1-4. SEM images of PLLA monoliths prepared from different 1,4-dioxane/2-butanone/water ratios [(a):85/0/15, (b):65/20/15, (c):45/40/15, (d):25/60/15].

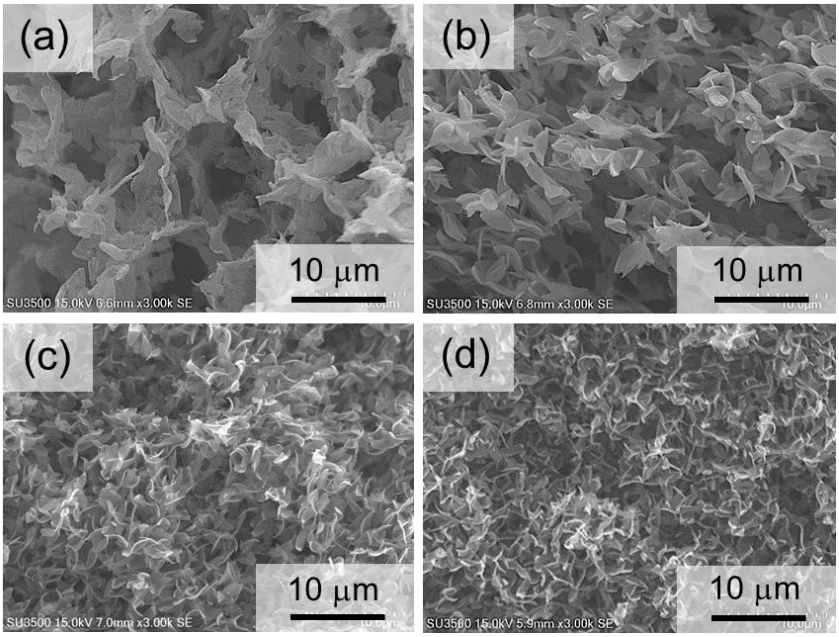

Figure 1-5. SEM images of PLLA monoliths prepared from different 1,4-dioxane/2-butanone/water ratios [(a):25/60/15, (b):20/70/10, (c):15/80/5, (d):10/90/0] with high resolution.

SEM images demonstrated that all samples exhibited 3D porous structure which was frozen by phase separation. Figure 1-4 clearly shows that the wall-like morphology was minimized self-similarly with increasing the ratio of 2-butanone at the range of (1,4-dioxane/2-butanone/water) 85/0/15-25/60/15 (v/v%) fixing water content. In addition, in the range of 25/60/15-10/90/0 (v/v%), with the collapse of wall-like morphology, pore and skeletal size in the PLLA monoliths were decreased dramatically with higher 2-butanone content and given unique morphology in which leaf-like small units were interconnected (Figure 1-5). This leaf-like structures can be considered as single PLLA crystals which are fabricated at the early stage of solid-liquid phase separation. These single crystals are known to be formed in the polymer rich phase at initial stage of solid-liquid phase separation within a limited condition.[5] From these SEM images, the averaged pore size of the monoliths was calculated by collecting each

pore diameters (Figure 1-6). Amazingly, the averaged pore size was diminished drastically from 28.6 μm to 1.1 μm by only changing the solvent ratio, where the skeletal size was also decreased from 2500 nm to less than 200 nm. These descents in size can also be explained by the speed of phase separation and the crystallization of PLLA mentioned above. The slower phase separation induced by higher content of 2-butanone promotes PLLA crystallization (see Table 1-1) that leads higher viscosity in the system and arrests phase separation in earlier stage, resulting in shorter gelation time and gel formation with minimized morphology.[5]

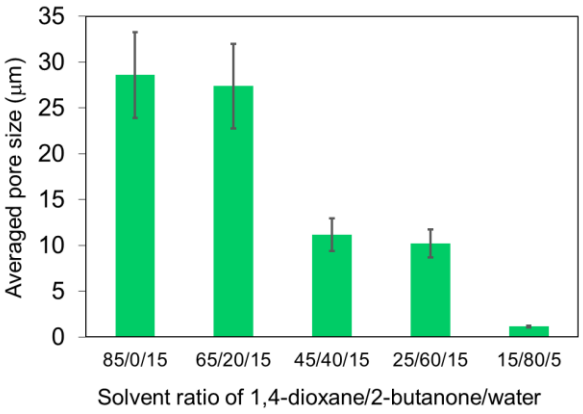

Figure 1-6. The change in averaged pore size of PLLA monoliths prepared at different 1,4-dioxane/2-butanone/water ratios calculated from SEM images shown in Figure 1-4 and 1-5.

For comparison with other controlling factors than the 2-butanone ratio, it was additionally investigated the effect of PLLA concentration on monolith formations (Figure 1-7).

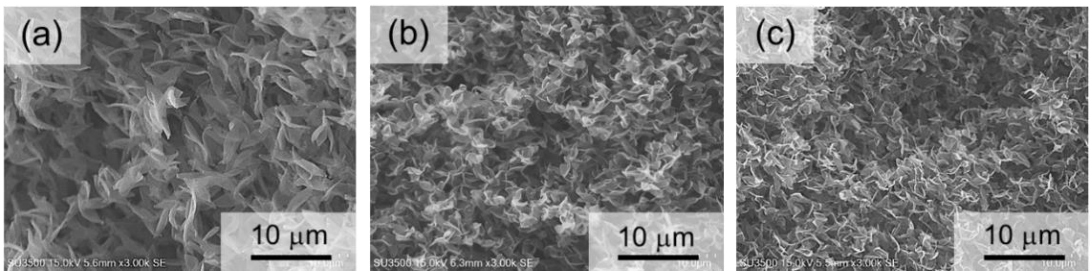

Figure 1-7. SEM images of PLLA monoliths prepared at (15/80/5) 1,4-dioxane/2-butanone/water with different PLLA concentration [(a):50 mg/mL, (b):100 mg/mL, (c):150 mg/mL].

PLLA monoliths were successfully produced at fixed (15/80/5) 1,4-dioxane/2-butanone/water ratio with the limited PLLA concentration of *ca.* 50-150 mg/mL, whereas that prepared from less than 50 or over 150 mg/mL resulted in polymer precipitate after quenching or heterogenous solution before the phase separation process. SEM observation clearly demonstrated that the leafy framework in the monoliths was minimized with increasing the concentration of PLLA, however, the change on morphology was occurred in narrow scope compared to the variations generated by 2-butanone content. This fact may indicate that the influence of the amount of 2-butanone on phase separation is more critical in the system than the change in PLLA concentration.

In the past, PLLA monoliths produced from common TIPS method using binary solvent tended to have micron scale of wall-like morphology because of the fast phase separation given by absence of the solvent which controls the phase separation and PLLA crystallization efficiently.[1,2] In the present study, PLLA monoliths having micron to nano meter scale of pore and skeletal sizes with leaf-like morphology were successfully produced by only changing the ternary solvent ratio using 2-butanone as the controlling factor of TIPS. It was demonstrated that the novel TIPS method using ternary solvent including 2-butanone is ideal for the synthesis of PLLA monoliths compared to the more commonly used binary solvent.

1.4 Conclusion

This work utilized for the first time that the TIPS using novel ternary solvent of 1,4-dioxane/2-butanone/water to fabricate PLLA monoliths with excellent

controllability in morphology. The influence of the addition of 2-butanone as a controlling factor was elucidated from the ternary phase diagram of the solvents and characterization of the resultant monoliths, focusing on the relationships between its structure and characteristics. It was demonstrated that 2-butanone in the 1,4-dioxane/water mixture significantly affects the morphology and crystallinity of PLLA monoliths. Furthermore, it was revealed that 2-butanone is capable of promoting the slow phase separation which leads the diminished structure. Besides, the addition of mid-solvent expands the selection of solvent condition, which enables precise control in morphology just by changing the ratio of the solvents without any controlling factors such as polymer concentration, molecular weight, and quenching temperature. The ternary phase diagram proposed for the TIPS in this study successfully explains the present results. The PLLA monoliths exhibited micron to nano scale of pore (28.6-1.1 μm) and skeletal (2500-200 nm) size with high porosity up to 90-93% were successfully obtained by only changing the starting solvent ratios during phase separation. Moreover, it was observed that the unique transition to interconnected leaf-like structure from wall-like morphology with increasing the content of 2-butanone. Thus, it was demonstrated that the PLLA monoliths with unique morphology and precise controllability in pore and skeletal size can be fabricated by newly developed TIPS.

1.5 References

1. Tanaka, T.; Lloyd, D. R. *J. Membr. Sci.* **2004**, 238, 65-73.
2. Önder, Ö. C.; Yilgöl, E.; Yilgöl, I. *Polymer* **2016**, 107, 240-248.
3. Fischer, E.W.; Sterzel, H.J.; Wegner, G. *Kolloid. -Z. Z. Polym.* **1973**, 251, 980-990.
4. Ma, P. X.; Zhang, R. Y. *J. Biomed. Mater. Res.* **1999**, 46, 60-72.
5. E. Rezabeigi, P. M. Wood-Adams, and R. A. L. Drew, Polymer, **2014**, 55, 6743.
6. Tanaka, T.; Eguchi, S.; Aoki, T.; Tamura, T.; Saitoh, H. Taniguchi, M. Ohara, H.; Nakanishi, K.; Lloyd, D. R. *Biochem. Eng. J.* **2007**, 33, 188-191.
7. Tanaka, T.; Nishimoto, T.; Tsukamoto, K.; Yoshida, M.; Kouya, T.; Taniguchi, M.; Lloyd, D. R. *J. Membr. Sci*. **2012**, 396, 101-109.
8. Mannella, G. A.; Pavia, F. C.; Carrubba, V. L.; Brucato, V. *Eur. Polym. J.* **2016**, 79, 176-186.
9. Nie, T.; He, M.; Ge, M.; Xu, J.; Ma, H. *Appl. Polym. Sci.* **2017**, 134, 44885-44895.
10. Xin, Y.; Fujimoto, T.; Uyama, H. *Polymer* **2012**, 53, 2847-2853.

Chapter 2.

Unique transitions in morphology and characteristics of monolithic poly(lactic acid) enantiomers

2.1 Introduction

A use of PLLA monolith has been attempted as scaffolds for cultivating human cell, artificial bones, matrices for drug delivery, and biodegradable filters with increasing demand and awareness to environmental conservation. However, its quite low thermal properties and chemical resistance are insufficient for the use mentioned above. For instance, a framework of PLLA monolith is easily collapsed with a sterilization using high-temperature steam (*ca*. 190 ^{o}C) because of its low melting temperature (*ca*. 170 ^{o}C) and glass transition (*ca*. 60 ^{o}C).[1] Moreover, PLLA monolith with high surface area can be dissolved instantly in a number of solvents, particularly at high temperature, which limits usage environments.

A formation of stereocomplex PLA (sc-PLA) between enantiometric PLLA and poly(D-lactic acid) (PDLA) is promising to improve thermal properties and chemical resistance, because the stereocomplex crystals exhibit not only higher melting temperature (*ca*. 230 ^{o}C) than homo-chiral (hc) crystals (*ca*. 180 ^{o}C) but also higher chemical resistance due to the strong hydrogen-bonding between PLLA and PDLA.[2] It was also reported that a high degree of stereocomplexation enables sc-PLA to achieve higher tensile strength and tensile modulus as high as 2-2.5 times compared to pristine PLLA.[3] In addition, for a medical use, a cell adhesion on a surface was improved by the

formation of sc.[4] Therefore, utilizing of stereocomplex would transform PLLA monoliths to a high-performance porous material, which can be used in various fields mentioned above with no difficulty. Although the formations of gel, particle, and porous surface using sc-PLA have been studied previously,[5-9] there has been no report so far that investigates a monolithic pure sc-PLA. Moreover, a phase separation technique combined with setereocomplexation between enantiometric polymers has not been developed for producing polymer monoliths despite the fact that a variety of monoliths are now mainly fabricated through phase separation because of its simplicity and processability. For example, recently, Gao *et al*. synthesized porous petal-like PLA surfaces using the stereocomplexation and demonstrated that the quasi super-hydrophobic PLA surface containing sc crystals exhibited a tunable adhesion force to water droplet.[9] However, the technique they conducted was entirely dedicated to produce thin PLA surface and may not be applied to tailor the monoliths for medical and filtration technologies mentioned above. Thus, until now, no approach has been studies with fabricating the pure sc-PLA monolith (without any hc crystals) nor fundamental researches on physical properties of the monolith.

In this chapter, the author focused on finding a route to produce highly porous PLA monoliths containing sc crystals having no hc crystals formed in single PLLA or PDLA using a simple phase separation technology developed in Chapter 1, elucidating a mechanism during the process. Furthermore, it was also attempted to reveal the relationships between structures and fundamental characteristics of sc-PLA monoliths.

2.2 Experimental

Materials

L,L-lactide and D,D-lactide were purchased from Tokyo Chemical Industry Co., Ltd. and Musashino Chemical Laboratory, Ltd., respectively. Tin(II) octoate was purchased from Wako Pure Chemical Industries, Ltd. 1-Octanol, dichloromethane, methanol, 1,4-dioxane, 2-butanone, 2-propanol (iPA), dimethyl sulfoxide (DMSO), chloroform, tetrahydrofuran (THF), acetonitrile, *N*-metyl-2-pyrolidone (NMP), and toluene were obtained from Nacalai tesque and were used as received.

Synthesis of PLLA and PDLA

PLLA and PDLA were synthesized through ring-opening polymerization using tin(II) octoate from L,L- and D,D-lactides (Figure 2-1). The weight-averaged molecular weights (M_w) of PLLA and PDLA were tailored under M_w = 1.0 x 10^5 g/mol since the blends of PLLA and PDLA with M_w higher than 1.0 x 10^5 g/mol are likely to form hc crystals rather than sc.[1]

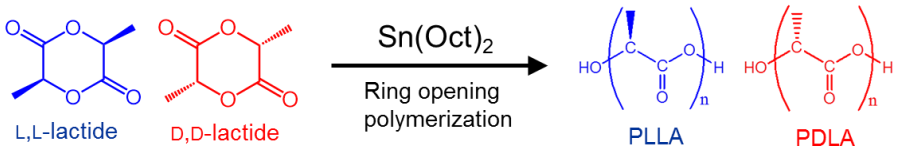

Figure 2-1. Synthesis of PLLA and PDLA in this study.

At first, L,L- and D,D-lactides were melted at 160 °C for 3 h under argon atmosphere in a presence of 0.1 mol% (*vs.* lactides) tin(II) octoate with 0.254 and 0.126 mol% (*vs.* lactides) of 1-octanol as a initiator, respectively. Then, the solution was continuously heated at 130 °C for 5 h followed by a heating under vacuum for 1 h. The resultant products were dissolved with 40 mL of dichloromethane at r.t., and precipitated in methanol. The obtained PLLA and PDLA were dried in vacuo for 6 h at r.t. Table 2-1 summarizes the physical properties of PLLA and PDLA prepared in this study.

Table 2-1. Characteristics of resultant PLLA and PDLA.

	M_n[a] (g/mol)	M_w[b] (g/mol)	T_g[c] (°C)	T_m[d] (°C)	X_c(hc)[e] (%)
PLLA	1.5 x 10^4	4.4 x 10^4	69	176	57
PDLA	2.4 x 10^4	8.2 x 10^4	63	177	52

a : M_n = number-average molecular weight.

b : M_w = weight-average molecular weight.

c : T_g = glass transition temperature.

d : T_m = melting temperature of PLLA crystal.

e : X_c(hc) = crystallinity of PLLA crystal calculated from DSC measurements assuming the theoretical heat of fusion = 93.1 J/g.[10]

Preparation of PLLA/PDLA monoliths

PLA monoliths with sc crystals were synthesized by thermally induced phase separation with ternary solvent: 1,4-dioxane as a good solvent, water as a non-solvent, and 2-butanone as a mid-solvent (Scheme 2-1).

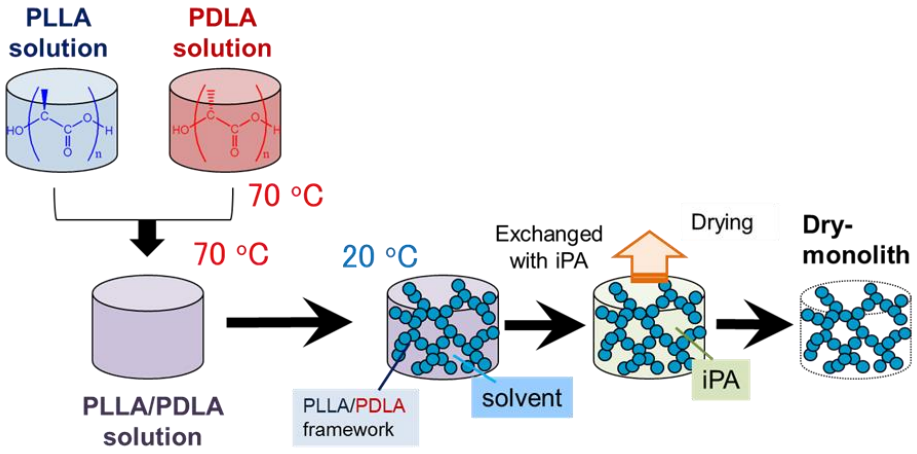

Scheme 2-1. Fabrication process of sc monoliths in this study.

A conditions of the mixed solvents were partially referred with examination conducted in Chapter 1. In short, 2-butanone in the 1,4-dioxane/water mixture critically affects a speed of phase separation and gelation time of the PLLA solution. The slower phase

separation induced by the addition of 2-butanone promotes crystallization of PLLA, which arrests de-mixing in an earlier stage (short gelation time) and diminish a pore structure compared to the traditional binary 1,4-dioxane/water system. At first, PLLA and PDLA were dissolved respectively in 1,4-dioxane/2-butanone mixture at 70 ^{o}C with the fixed PLA concentration of 100 mg/mL for 30 min. Then, water was added to the solution fixing the specific solvent ratio to (1,4-dioxane/2-butanone/water) 45/40/15 (v/v%) and stirred for 10 min to give clear solution. The PLLA and PDLA solutions were mixed in a range of (PLLA/PDLA) 100/0-0/100 (v/v%) at 70 ^{o}C followed by stirring for 2 min. The solution was immediately cooled to 20 ^{o}C overnight to induce phase separation. The resultant gels were exchanged to iPA followed by placing in a vacuum and dried at r.t. for 5 h to yield PLA dry-monoliths.

Analysis

Gel permeation chromatography (GPC) was carried out to determine a number-average and weight-average molecular weight (M_n and M_w, respectively) of the resultant PLLA and PDLA by a SC8020 apparatus (Tosoh Co.) with a reflective index (RI) detector and a TSKgel G5000HR column using chloroform as eluent at a flow rate of 1.0 mL/min. Calibration curve for GPC analysis was obtained using polystyrene standards. Melting temperature (T_m), and crystallinity (X_c) of the PLA monoliths and their starting PLLA/PDLA polymers were estimated by differential scanning calorimetry (DSC) using a SEIKO DSC6220, in a range between 50 and 250 ^{o}C at a heating rate of 10 ^{o}C/min and a nitrogen flow rate of 50 mL/min. The crystallinity of the homo-chiral (hc) and sc crystals were calculated using the theoretical heat of fusion (hc: 93.1 J/g, sc: 142 J/g).[10,11] Morphology of PLLA/PDLA monoliths were observed by scanning electron microscope (SEM) using a HITACHI SU-3500 instrument. N_2

adsorption/desorption isotherms for the PLLA/PDLA monoliths were measured using a NOVA-4200e surface area & pore size analyzer (Quantachrome Instruments) at 77 K. Regarding the N_2 sorption test, Brunauer-Emmett-Teller method (BET) and Barrett-Joyner-Halenda method (BJH) were used to calculate the specific surface area and pore volume of PLLA/PDLA monoliths, respectively. Chemical-resistances of the neat PLLA and the sc-PLA monolith were observed by a soaking test using PLA good solvents. The monoliths were soaked in good solvents of PLLA with degassing by a pump to remove the air inside the monoliths, followed by slow stirring for 1 week. Contact angle (CA) test was performed by a Drop Master DM300 instrument (Kyowa Interface Science) using a FAMAS Basic software. CA was measured 8 times for each sample with 1.5 μL of water to calculate average CA.

2.3 Results and discussion

Morphological transition of PLLA/PDLA monoliths

PLA monoliths were successfully produced without undergoing shrinkage in the all range of PLLA/PDLA from the ternary solvent of (1,4-dioxane/2-butanone/water) 45/40/15 (v/v%). Other choice of the solvent ratios and quenching temperatures resulted in polymer precipitation or clear solution without gelation at specific range in PLLA/PDLA during the phase separation process, whereas the only system of (1,4-dioxane/2-butanone/water) 45/40/15 and cooling temperature (70 ^{o}C to 20 ^{o}C) could produce PLA monoliths without shrinkage after gelation throughout the PLLA/PDLA ratio of 100/0-0/100 (v/v%). Therefore, at this conditions, it can be comparably discussed with the effect of PLLA/PDLA ratio against monolith structures and physical properties. The resultant samples were analyzed by SEM, DSC

and N_2 sorption test to elucidate the relationships between porous structures and characteristics of the monoliths.

The SEM observation revealed that all samples exhibited 3D interconnected structure without any independent pore throughout the monoliths (Figure 2-2A). It is interesting to note that a basic structure of the monoliths was gradually changed by the ratio of PLLA/PDLA: The monolith prepared from pristine PLLA showed a needle-like morphology, whereas that prepared from (50/50) PLLA/PDLA exhibited a spherical structure (Figure 2-2B).

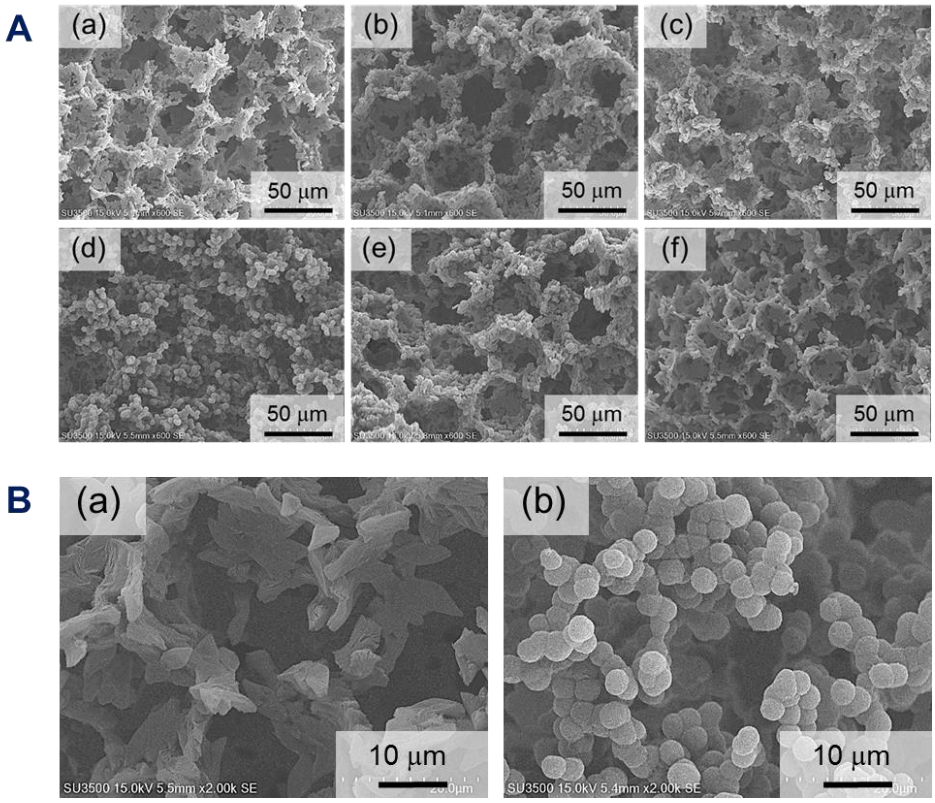

Figure 2-2. (A): SEM images of monoliths prepared at different PLLA/PDLA ratios [(a): 100/0, (b): 80/20, (c): 70/30, (d): 50/50, (e): 30/70, (f): 0/100]. (B): Change in morphology of PLLA/PDLA [(a): 100/0, (b): 50/50] with high resolution.

It is also demonstrated that these needle and round units were co-existed in the monolith fabricated at the PLLA/PDLA ratio between 80/20-70/30. Moreover, the morphology of

monoliths were changed back to needle-like with increasing the PDLA ratio over equivalence. These phenomena are occurred probably due to the stereocomplexation of PLLA/PDLA and the difference in speed of crystallization between sc and hc. During the cooling process of PLA solution, the gelation caused by liquid-liquid and solid-liquid phase separations can be occurred competitively.[12,13] As described in general introduction, it is commonly known that liquid-liquid phase separation generates a 3D porous structure *via* spinodal decomposition (de-mixing between polymer rich and lean phase), while solid-liquid phase separation gives a sea-island morphology including polymer precipitation by crystallization.[14,15] In this case, solid-liquid phase separation may be promoted simultaneously after with liquid-liquid phase separation caused by temperature reduction.[16] That is, the crystallization of hc and sc may take place in the polymer rich phase within liquid-liquid phase separation, which leads to the porous morphology having hc and sc crystals. Few studies have been conducted that examine the needle-like PLLA crystals utilizing close solvent conditions used in this study.[13,16] In the same manner with the leaf-like crystals in Chapter 1, these needle-like structures can be single PLLA crystals produced at the initial stage of solid-liquid phase separation. In contrast, sc crystals are formed prior to the crystallization of neat PLLA or PDLA because of the rapid crystallization rate of sc compared with that of hc.[17,18] Chang *et al*. reported that spherical sc structures can be formed using a phase separation process because sc lamellae grow parallel along a interface between a polymer-rich droplet and solution during solid-liquid phase separation.[18] Hence, the rapid formation of sc particles prior to the hc crystals during solid-liquid phase separation can lead to the morphology with spherical units or double units of sc and hc depending on the PLLA/PDLA ratio.

Physical properties of PLLA/PDLA monoliths

Next, the DSC measurements were carried out to investigate the heat resistance and sc crystallinity in the PLA monoliths (Figure 2-3).

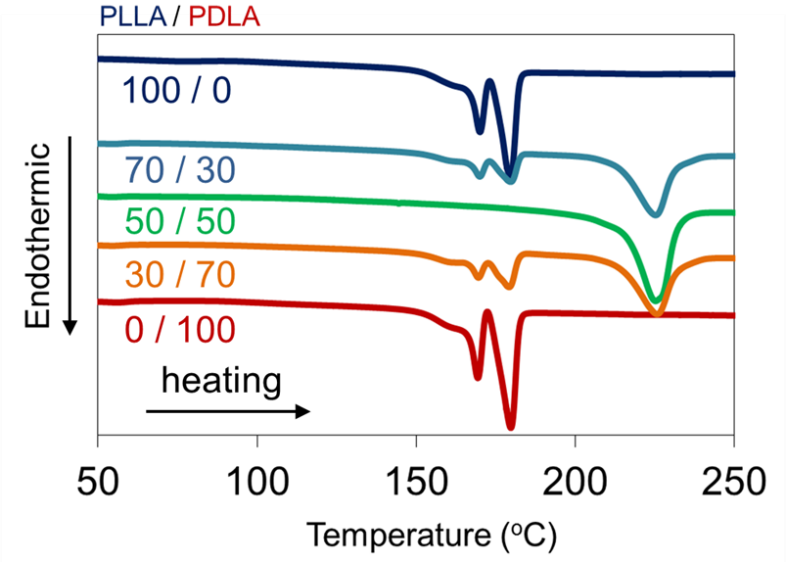

Figure 2-3. DSC thermograms of monoliths prepared from different PLLA/PDLA ratios.

The melting temperature (T_m) peaks split into 170 °C and 180 °C are corresponding to α' and α crystals of hc, respectively.[19,20] The T_m peaks of hc crystals disappeared when reaching the PLLA/PDLA ratio to equivalence, and only the T_m of sc crystals appeared in (50/50) PLLA/PDLA monolith at ca. 50 °C higher than the former T_m. This tendency is clearly tracing the morphological transition observed above. From a calculation using the theoretical heat of fusion (hc: 93.1 J/g, sc: 142 J/g),[10,11] the sc-crystallinity of the monolith prepared at the stoichiometric amount of PLLA/PDLA reached to 53% (Table 2-2). It is noteworthy that the crystallinity of the pristine PLLA and PDLA monoliths were much higher than the starting PLLA/PDLA oligomers used for the synthesis (Table 2-1). This tendency has been discussed previously[13] that a higher PLA crystallinity can be achieved by the ordering and crystallizing of PLLA chains during slow phase

separation induced by 1,4-dioxane/2-butanone/water system.

Table 2-2. Physical properties of PLLA monoliths prepared at different PLLA/PDLA ratios.

PLLA/PDLA	T_m(hc(α'))[a] (°C)	T_m(hc(α))[b] (°C)	T_m(sc)[c] (°C)	X_c(hc)[d] (%)	X_c(sc)[e] (%)
100/0	169	180	-	68	-
70/30	170	179	226	24	33
50/50	-	-	226	-	53
30/70	170	180	226	29	32
0/100	170	180	-	71	-

a : T_m(hc(α')) = melting temperature of α' type hc crystal.

b : T_m(hc(α)) = melting temperature of α type sc crystal

c : T_m(sc) = melting temperature of sc crystal.

d : X_c(hc) = crystallinity of hc crystal calculated from DSC measurements assuming the theoretical heat of fusion = 93.1 J/g.[10]

e : X_c(sc) = crystallinity of sc crystal calculated from DSC measurements assuming the theoretical heat of fusion = 142 J/g.[11]

The N_2 sorption measurements by Brunauer-Emmett-Teller multi-plot method (BET) revealed that the monolith fabricated at (50/50) PLLA/PDLA had much higher specific surface area as high as 131 m^2/g compared to that prepared from neat PLLA (86 m^2/g) (Figure 2-4). Furthermore, Barrett-Joyner-Halenda method (BJH) demonstrated that the pore volume of the sc monolith was also higher (0.37 cc/g) than that of pristine PLLA (0.30 cc/g), which clearly indicates the great number of mesopores in the monolith prepared at the stoichiometric amount of PLLA/PDLA. This is probably

because of the hierarchical structure of the sc monolith having a coarse surface of sc particles.[26] Therefore, it is demonstrated that the stereocomplexation gives a considerable increase in surface area to PLA monoliths, which can be valuable for a precise control of PLA pore structures.

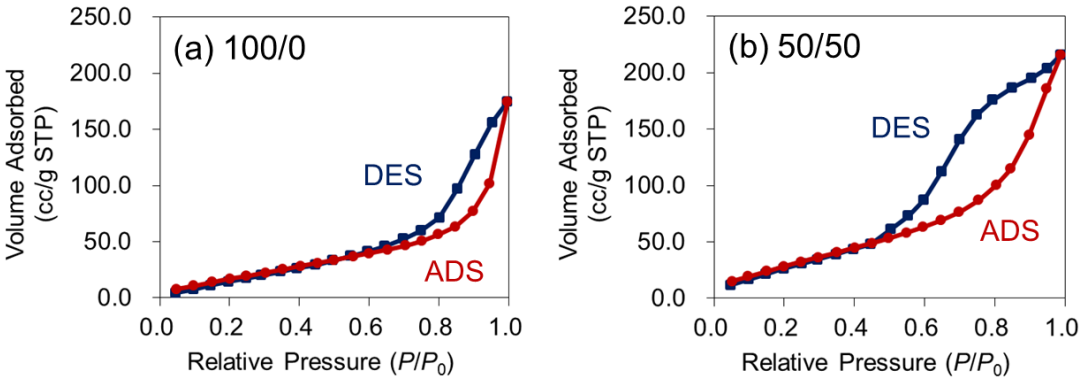

Figure 2-4. N_2 adsorption(ADS)-desorption(DES) isotherms of the monolith prepared at different PLLA/PDLA ratios [(a): 100/0, (b): 50/50]

The chemical-resistance of the PLA monoliths was investigated by a soaking test (Figure 2-5A). In this examination, the PLA monoliths were soaked in PLA good solvents listed in Table 2-3 for 1 week with stirring.

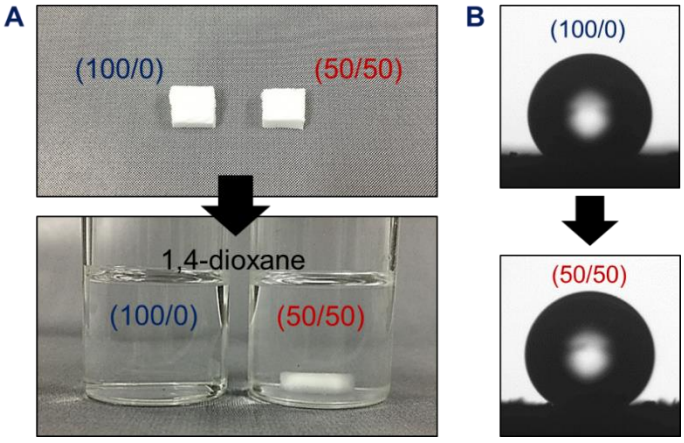

Figure 2-5. (A) Photo images of monoliths prepared from PLLA/PDLA [Left: 100/0, Right: 50/50] soaked in 1,4-dioxane for 1 week; (B) Quasi super-hydrophobic surface of sc-PLA monolith observed by con-tact angle test [Top: PLLA/PDLA (100/0), Bottom: (50/50)].

Table 2-3. Result of soaking test* and good solvents of PLLA.

1,4-dioxane	○	THF (50 °C)	○
DMSO (80 °C)	○	acetonitrile (70 °C)	○
dichloromethane	X	NMP (90 °C)	○
chloroform	X	toluene (90 °C)	○

*The monolith prepared from (50/50) PLLA/PDLA was [○: insoluble, X: collapsed] to these solvents.

The monolith prepared from the pristine PLLA dissolved instantly in the good solvents of PLA. However, the monolith prepared from (50/50) PLLA/PDLA exhibited excellent resistance to most of these solvents, and argued that the high degree of sc formation enabled PLA monolith to achieve higher chemical-resistance. It is well known that a higher stability of sc crystals leads better chemical-resistance than that of hc because of the intermolecular hydrogen bonding between enantiometric PLLA/PDLA and the dense chain packing.[1,21] Regarding dichloromethane and chloroform, the sc monolith was collapsed with these solvents within an hour probably because of the weak physical connection between the sc particles (see Figure 2-2B).

Finally, per the aforementioned chemical-resistance, a contact angle test was performed to elucidate a change in hydrophobicity of the PLA monoliths after the stereocomplexation (Figure 2-5B). The monolith fabricated from 50/50 (PLLA/PDLA) exhibited significantly high water contact angle up to $144.5^{o} \pm 1.5^{o}$, whereas the neat PLLA monolith showed relatively low angle ($137.5^{o} \pm 2.1^{o}$). The improvement in hydrophobicity may be due to both the formation of sc mentioned above and the coarser morphology of the monolith (see Figure 2-2). In the previous study, Gao *et al*. also reported a high hydrophobic PLA surface (membrane) with the water contact angle

between 140-145^{o} using different PLLA/PDLA ratio (7/3).[9] In this study, it was successfully tailored the PLA monolith with the quasi super-hydrophobic surface from the equal ratio of PLLA/PDLA *via* simple phase separation method using ternary solvent.

2.4 Conclusion

In this chapter, it was reported for the first time that the unique transitions in morphology and fundamental physical properties of the porous PLA enantiomers in addition to its fabrication method using thermally induced phase separation. The PLA monoliths with sc crystals were successfully prepared by enantiometric PLLA and PDLA through simple phase separation using the ternary solvent (1,4-dioxane/2-butanone/water). It was clearly observed that the frameworks of the monoliths were changed drastically by the ratio of PLLA/PDLA. The PLA monolith prepared from neat PLLA or PDLA showed the interconnected needle-like morphology, whereas that prepared from PLLA/PDLA (50/50) exhibited the spherical structure. The PLA monolith prepared at equal ratio of PLLA/PDLA had high sc-crystallinity as high as 53% without any hc crystals, and it showed much higher melting temperature (226 ^{o}C), surface area (131 m^2/g), and static water contact angle (144.5^{o}) than those of neat PLLA (180 ^{o}C, 86 m^2/g, 137.5^{o}, respectively). In addition, the monolith prepared from stoichiometric amount of PLLA/PDLA exhibited the excellent resistance to most of PLLA good solvents even for weeks. Thus, it was demonstrated for the first time that the PLA monoliths with high surface area, heat resistance, chemical-resistance, and even hydorophobicity can be fabricated through both the simple phase separation technology and stereocomplexation.

2.5 References

1. Isama, K. In Bio materials and medical devices - Approach to the safety and Bio compatibility, Eds.; CMC Publishing Co., Ltd: Japan, **2003**; p 25.
2. Tsuji, H. *Macromol. Biosci*. **2005**, 5, 569-597.
3. Tsuji, H. Ikada, Y. *Polymer* **1999**, 40, 6699-6708.
4. Watanabe, J.; Eriguchi, T.; Ishihara, K. *Biomacromolecules* **2002**, 3, 1375-1383.
5. Mao, H.; Pan, P.; Shan, G.; Bao, Y. *J. Phys. Chem. B.* **2015**, 119, 6471-6480.
6. Mao, H.; Shan, G.; Bao, Y.; Wu, Z. L.; Pan, P. *Soft Matter* **2016**, 12, 4628-4637.
7. Bibi, G.; Jung, Y.; Lim, J. C.; Kim, S. H. *ACS Sustainable Chem. Eng.* **2016**, 4, 4521-4528
8. Uehara, H.; Ishizuka, M.; Tanaka, H.; Kano, M.; Yamanobe, T. *RSC Adv.* **2016**, 6, 13971-13980.
9. Gao, A.; Zhao, Y.; Yang, Q.; Fu, Y.; Xue, L. *J. Mater. Chem. A.* **2016**, 4, 12058-12064.
10. Fischer, E. W.; Sterzel, H. J.; Wegner, G. *Kolloid. -Z. Z. Polym.* **1973**, 251, 980-990.
11. Loomis, G. L.; Murdoch, J. R.; Gardner, K.H. *Polym. Prepr.* **1990**, 31, 55-56.
12. Önder, Ö. C.; Yilgöl, E.; Yilgöl, I. *Polymer* **2016**, 107, 240-248.
13. Rezabeigi, E.; Wood-Adams, P. M.; Drew, R. A. L. *J. Polym. Sci. B Polym. Phys.* **2017**, 55, 1055-1062.
14. Lloyd, D. R. Kim, S. S.; Kinzer, K. E. *J. Membr. Sci.* **1991**, 64, 1-11.
15. Lloyd, D. R.; Kinzer, K. E.; Tsung, H. S. *J. Membr. Sci.* **1990**, 52, 239-261.
16. Rezabeigi, E.; Drew, R. A. L.; Wood-Adams, P. M. *Ind. Eng. Chem. Res.* DOI: 10.1021/acs.iecr.7b02786.
17. Tsuji, H.; Ikada, Y. *Macromolecules* **1993**, 26, 6918-6926.

18. Chang, X.; Bao, J.; Shan, G.; Bao, Y.; Pan, P. *Cryst. Growth Des.* **2017**, 17, 2498-2506.

19. Tábi, T.; Hajda, S.; Kovács, J. G. *Eur. Pol. J.* **2016**, 82, 232-243.

20. Pan, P.; Zhu, B.; Kai, W.; Dong, T.; Inoue, Y. *Macromolecules* **2008**, 41, 4296-4304.

21. Pan, P.; Bao, J.; Han, L.; Xie, Q.; Shan, G.; Bao, Y. *Polymer* **2016**, 98, 80-87.

Chapter 3.

Ivy-like morphology composed of poly(lactic acid) and bacterial cellulose cryogel

3.1 Introduction

Recently, PLA monolith has been in the spotlight as a functional material because of its high surface area and interpenetrating 3-D network. Owing to these unique characteristics, monolithic PLA has been utilized as scaffolds for human cells, artificial bones, supports for controlled release of drugs, and biodegradable filters as mentioned in general introduction. However, the practical use of PLA monoliths remains challenging because its mechanical properties considerably deteriorate due to the development of porous structures.[1] Furthermore, hydrophobic surfaces of monoliths that are notably high limit their applications, particularly in scaffolds and filters, because the loss of hydrophilicity produces insufficient medium osmosis and high back pressure during flow.[2] To overcome these drawbacks, numerous studies have been conducted to utilize modifier agents.[1,3,4] However, no studies far have achieved sufficient properties or were able to control the pore size. In particular, the precise control of pore size is critical to meeting requirements for usage, because the morphology of monoliths affects several factors such as cell adhesion, biodegradability, and filtration ability.[5] Thus, producing hydrophilic PLA monoliths that have high mechanical properties and enable the morphology to be controlled is desirable.

Bacterial cellulose (BC) gel can be a promising means to address the physical

properties and hydrophobicity of PLA monoliths. BC gel is an extracellular by-product of acetic acid bacteria, which exhibits biodegradability and biocompatibility similar to those of PLA.[6,7] Compared to general plant-based cellulose, BC gel has considerable superiority in terms of 3-D network, porosity, purity, crystallinity, and water content, making it an attractive biomaterial in numerous fields.[7-9] In addition, a layered structure is formed in a BC gel during cultivation, which is cause of its unique mechanical anisotropy.[10,11] Since it exhibits high Young's modulus, tensile, and compressive strength, BC gel has also been used to reinforce polymers.[12,13] Therefore, use of BC gel would change PLA monoliths to a next-generation porous material, storing its environmental adaptability.

Few studies have been conducted that examine PLA monoliths that use a single crystal of BC (i.e., BC nano-whisker (BCNW)) [14] instead of BC gel. In contrast to a BC gel with a 3D structure, BCNW can be easily introduced into PLA monoliths through a variety of methods. For instance, Luo *et al*. reported that poly(L-lactic acid) (PLLA) monoliths with 5 wt% of BCNW were successfully produced by a solvent casting method, which showed improved mechanical strength and hydrophilicity of PLLA monoliths.[14] However, mechanical properties showing increase in tensile strength, tensile modulus, and compressive strength were limited to less than 64% from the neat PLLA monolith. Furthermore, in contrast to BC gel, the addition of considerable BCNW generally causes self-aggregation, which causes poor dispersion. Thus, the amount of BCNW can be manipulated within a very narrow range in order to control physical properties and wettability.[15] In addition, until now, no studies have been conducted that achieved both the reinforcements previously mentioned and control of PLA porous morphology.

In this chapter, the author attempted to synthesize a monolithic composite of PLLA and BC gel with good mechanical strength and hydrophilicity *via* simple phase separation technique while controlling the porous morphology during the process. Moreover, it was conducted to measure the fundamental physical properties of the monoliths through a compressive test and a water contact angle examination. The mechanical anisotropy of the BC/PLLA monoliths was also investigated, focusing on the directions of BC layers.

3.2 Experimental

Materials

PLLA was purchased from NatureWorks LLC (Ingeo^{TM} Biopolymer 4032D). 1,4-Dioxane, and 2-butanone were obtained from Nacalai Tesque and were used as received. BC gel was purchased as a Nata De Coco from Thailand and exchanged with sufficient amount of water before use.

Preparation of BC/PLLA monoliths

BC/PLLA monoliths were prepared through the formation of a porous structure of PLLA within the BC gel using a thermally induced phase separation (TIPS) method. Utilizing TIPS has remarkable advantages in terms of process flexibility, reproducibility, and controlling the pore size when compared to the traditional non-solvent induced phase separation (NIPS).[16-18] For this study, the NIPS technique could not be used because its fast phase separation after non-solvents are added halts the diffusion of non-solvents in BC gel, thereby preventing PLLA from forming inside the gel. This suggests that TIPS can be a limited means to producing a monolithic BC/PLLA, while maintaining the morphology of each. TIPS was performed using 1,4-dioxane as a good

solvent, water as a non-solvent, and 2-butanone as a mid-solvent (Scheme 3-1).

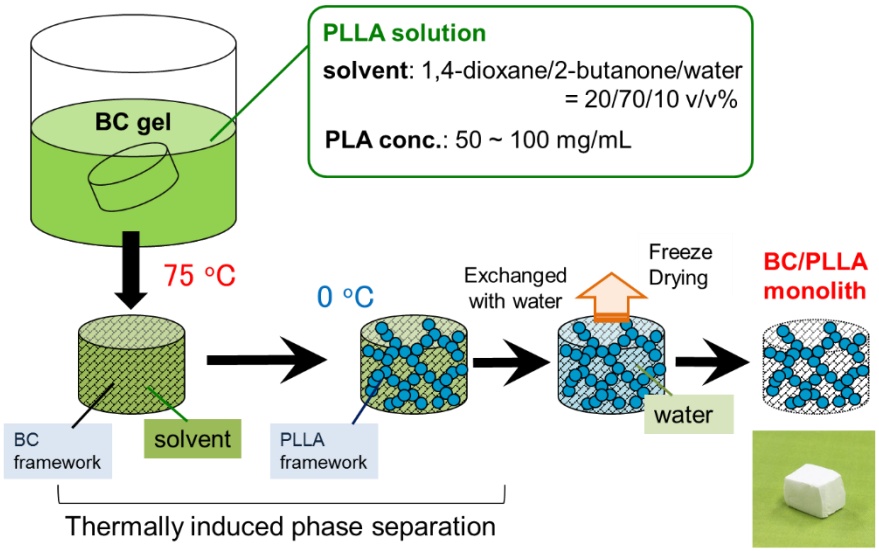

Scheme 3-1. Fabrication process of BC/PLLA monoliths in this study.

This recipe for the phase separation was based on the investigation in Chapter 1. Briefly, this ternary system that includes a mid-solvent easily enables PLLA morphology to be manipulated simply by changing the ratio of solvents or the concentration of PLLA

First, BC gel (water content = 99.5%) was immersed in 1,4-dioxane/2-butanone mixture at r.t., while fixing the solvent ratio (1,4-dioxane/2-butanone/water) to 20/70/10 (v/v%) with stirring overnight. PLLA was added to the solution in a range of 50-100 mg/mL (Table 3-1) and heated at 75 ºC for 20 h to produce a BC gel saturated with PLLA solution. Then, the BC gel that includes the PLLA solution was immediately cooled to 0 ºC for 1 h using an ice bath in order to induce phase separation of PLLA. The resultant BC/PLLA wet gel was exchanged with sufficient amount of water and was freeze-dried under 10 Pa for 2 d to yield BC/PLLA dry monoliths. Pristine PLLA monoliths listed in Table 3-1 were also prepared using this same method with fixed (1,4-dioxane/2-butanone/water) 20/70/10 (v/v%) as the solvent. Each sample was named BC/PLLA*x* or PLLA*x*, where *x* denotes the starting concentration of PLLA used.

Table 3-1. Basic properties of PLLA and BC/PLLA monoliths.

Sample name	PLLA conc.[a] (mg/mL)	Apparent density (g/cm^3)	BC content [b] (wt%)
PLLA50	50	NA*	-
PLLA75	75	NA*	-
PLLA100	100	0.096 ± 0.008	-
BC/PLLA50	50	0.058 ± 0.002	8.6 ± 0.3
BC/PLLA75	75	0.081 ± 0.001	6.1 ± 0.4
BC/PLLA100	100	0.107 ± 0.011	4.4 ± 0.3

a : PLLA concentration of the solution used in the phase separation process.

b : BC content in the PLLA/BC monolith calculated from the weight of starting BC gel assuming the water content of the gel = 99.5 wt%.

*NA : The specimens were collapsed during the measurements so that the data were not available.

Analysis

BC content in the PLLA/BC monolith was calculated using the weight of the starting BC gel assuming the water content of the gel was 99.5 wt% (n = 3). The morphology of the monoliths were observed through a scanning electron microscope (SEM) using a HITACHI SU-3500 instrument. Crystallinity (X_c) of the monoliths was estimated through differential scanning calorimetry (DSC) using SEIKO DSC6220, within a range of between 40 and 200 ^oC at a heating rate of 10 ^oC/min and a nitrogen flow rate of 50 mL/min. The crystallinity of the PLLA crystals was calculated using the theoretical heat of fusion (93.1 J/g).[19] N_2 adsorption isotherms for the monoliths were measured using a NOVA-4200e surface area & pore size analyzer (Quantachrome Instruments) at 77 K. The specific surface area of the monoliths was estimated using the

BET method. Our compressive test was conducted using an EZ Graph (Shimadzu) with a compression speed of 1 mm/min under 70% strain of the monoliths. The cuboid specimen (approximately 0.7 x 0.7 x 1.2 mm) was compressed parallel or perpendicularly to the BC layers (n = 3). The contact angle (CA) test was performed using a Drop Master DM300 instrument (Kyowa Interface Science) with FAMAS Basic software. CA was measured parallel to the BC layers with 2 μL of water to calculate the average CA (n = 3). To observe the absorbability of the monolith, the change in CA was also measured at 0.1, 1.0, 3.0, 5.0, 10, 20, 30, 40, 50, and 60 s after drop formation.

3.3 Results and discussion

Morphology of BC/PLLA monoliths

BC/PLLA monoliths were successfully prepared without undergoing shrinkage through freeze-drying. The overall BC content in the monolith was changed from 4.4 and 8.6 wt% as a result of the starting PLLA concentration (Table 3-1). The PLLA concentration of less than 50 or more than 125 mg/mL resulted in polymer precipitation without gelation or a clouded heterogeneous solution. In addition, PLLA50 and PLLA75 were sufficiently fragile to be collapsed before sample forming or measurements.

SEM observation demonstrated that the open-porous BC/PLLA structure was formed without discontinuous pores (Figure 3-1) storing the original anisotropy of BC (Figure 3-2). It is noteworthy that the BC/PLLA monoliths exhibited an ivy-like double network (Figure 3-3) composed of BC fiber (Figure 3-1a) and a leaf-like PLLA unit (Figure 3-1b,c). Furthermore, a single PLLA unit was also formed and attached to the BC framework, which is clearly seen in BC/PLLA50 (Figure 3-1d). This suggests that

crystallization of PLLA occurred in the BC gel through solid-liquid phase separation during the TIPS process, and is the main mechanism of the formation.

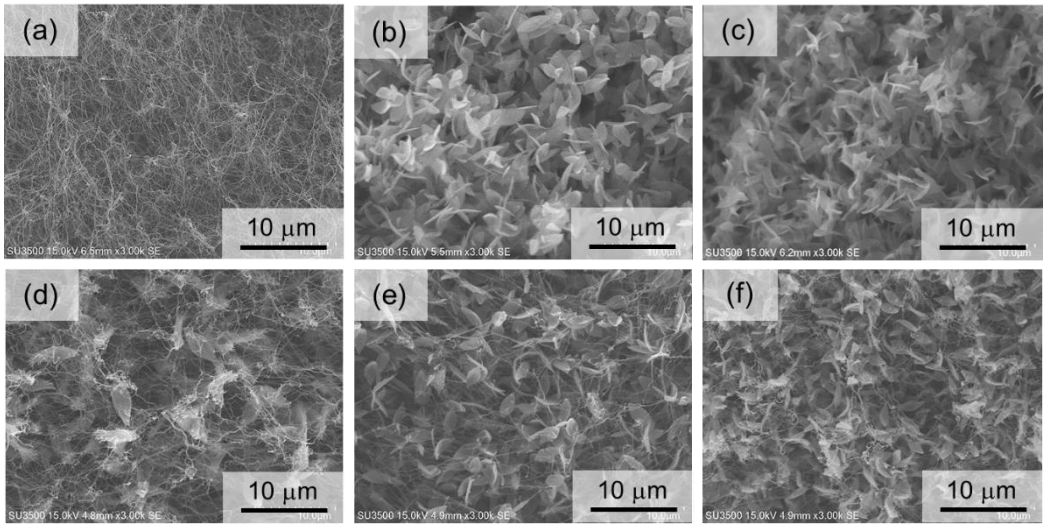

Figure 3-1. SEM images of BC, PLLA, and BC/PLLA monoliths [(a): BC cryogel, (b): PLLA75, (c): PLLA100, (d): BC/PLLA50, (e): BC/PLLA75, (f): BC/PLLA100].

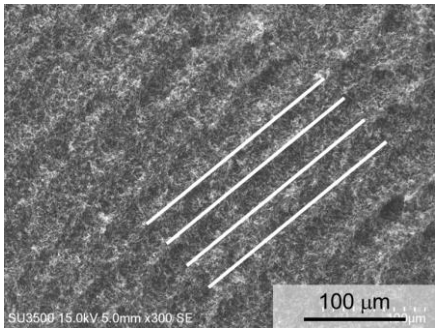

Figure 3-2. SEM image of anisotropic BC/PLLA75.

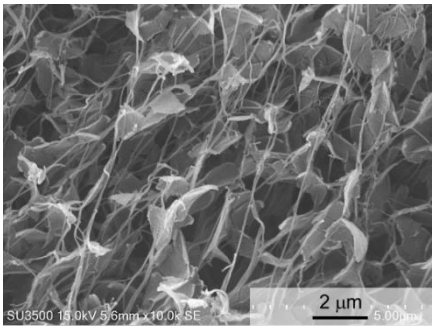

Figure 3-3. Ivy-like morphology of BC/PLLA100 observed by SEM analysis.

Considering the formation of a leaf-like PLLA 3D network and the existence of an independent PLLA unit, the crystallization of PLLA (solid-liquid phase separation) can occur during the polymer-rich phase of initial liquid-liquid phase separation induced by quenching. This tendency can be found in studies on PLLA monoliths (e.g., Rezabeigi *et al*. also successfully fabricated non-continuous porous PLLA through solid-liquid phase separation through NIPS).[20,21] The leaf-like PLLA unit found in this study may be

explained by the formation of single PLLA crystal formed at the beginning of the solid-liquid phase separation. As described in Chapter 1, It is known that PLLA monoliths consisting of leaf- or lozenge-like crystals can be prepared through both TIPS and NIPS under limited conditions.[20,21] Per the previous discussion, DSC measurements (Figure 3-4) were carried out to calculate the crystallinity (X_c) of PLLA assuming a theoretical heat of fusion of 93.1 J/g.[19] The X_c of BC/PLLA100 (66%, PLLA section) and PLLA100 (68%) monoliths were much higher than that of the starting PLLA pellet (39%), which clearly suggests that the crystallization of PLLA was promoted by solid-liquid phase separation. In particular, the X_c of BC/PLLA100 was significantly high despite the presence of BC fiber in the PLLA framework. This was probably because BC fiber acted as a nucleating agent for PLLA during phase separation.[22] For this reason, the crystallization of PLLA could start at the surface of the BC fiber, resulting in ivy-like morphology in which leaf-like PLLA crystals are entangled within the BC network. It is interesting to note that the size of leaf units was minimized when the content of PLLA was increased (see Figure 3-1). This was because of the higher viscosity induced by both dense concentration and fast crystallization of PLLA, which limited the initial liquid-liquid phase separation and induces minimized crystal morphology.[5] This suggests that the pore size and surface morphology can be manipulated by the starting PLLA concentration. To evaluate how easily the morphology can be controlled, a BET N_2

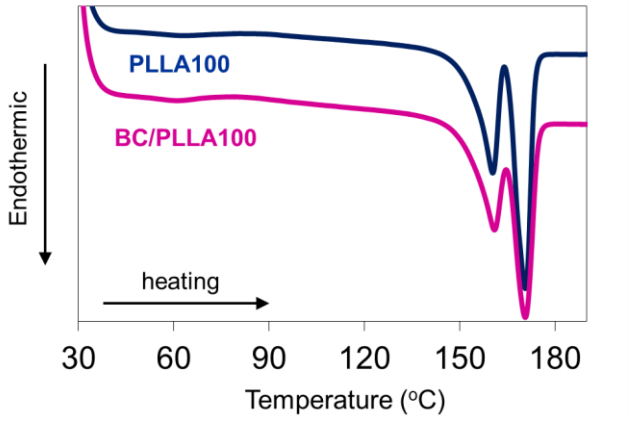

Figure 3-4. DSC thermograms of BC/PLLA100 and PLLA100.

adsorption test was performed (Figure 3-5, Table 3-2), which revealed that the specific surface area of the BC/PLLA monolith decreased with increasing amounts of PLLA.

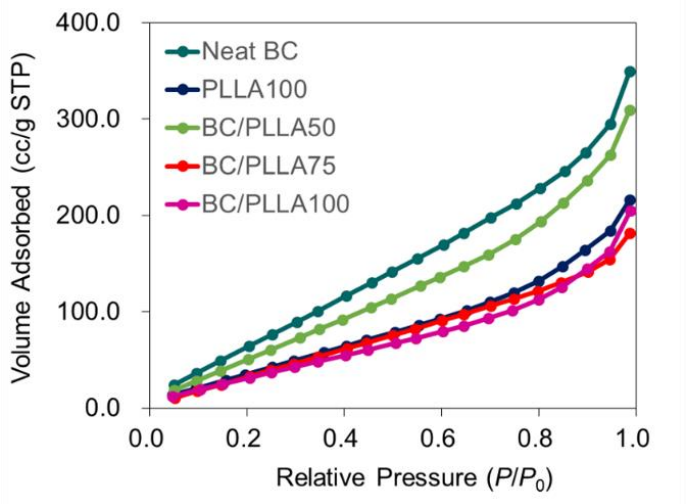

Figure 3-5. N_2 adsorption isotherms of PLLA and BC/PLLA monoliths.

Table 3-2. Mechanical properties of BC/PLLA monoliths.

Sample name	Maximum stress[a] (MPa)	Specific surface area [b] (m^2/g)	Contact angle[c] (°)
Neat BC	NA*	384.2	NA*[2]
PLLA100	0.52 ± 0.01	212.1	128.8 ± 1.1
BC/PLLA50	0.53 ± 0.04[a], 0.49 ± 0.04[b]	316.2	102.1 ± 1.7
BC/PLLA75	1.12 ± 0.02[a], 0.92 ± 0.04[b]	225.8	NA*[2]
BC/PLLA100	2.12 ± 0.13[a], 2.12 ± 0.08[b]	176.2	NA*[2]

a : Maximam stress at 70% strain of monoliths determined by compression test. Superscript notations of α and β are denoted the directions of compression [α: parallel to BC layers, β: perpendicular to BC layers].

b : Specific surface area determined by N_2 adsorption test using BET method.

c : Static water contact angle measured on monoliths at 0.1 s after drop parallel to BC layers.

*NA : The monolith was collapsed during sample forming so that the data were not available.

*[2]NA : The specimen rapidly adsorbed water so that the data were not available.

This was possibly due to the relatively flat surface of the PLLA unit (Table 3-2) and the change in PLLA surface structure caused by phase separation in the presence of BC. Therefore, it is demonstrated that the ivy-like BC/PLLA monoliths with highly porous morphology and good controllability of pore size could be effectively tailored using a simple TIPS technique.

Mechanical properties of BC/PLLA monoliths

Next, the compressive test was performed to examine the change in mechanical strength of BC/PLLA monoliths (Figure 3-6, Table 3-2). The sample was compressed perpendicularly or parallel to the BC layers in order to measure the mechanical anisotropy of the monoliths. It was surprising that the BC/PLLA100 exhibited four times higher compressive stress than the PLLA100 at 70% strain (Figure 3-6A, Table 3-2) although dried neat BC gel has critical fragility.[23,24]

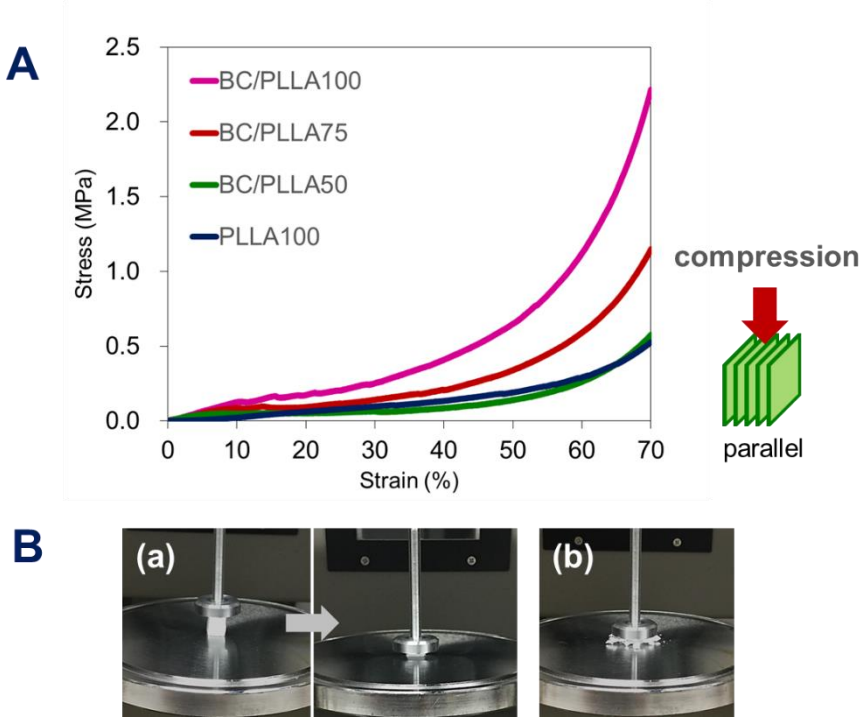

Figure 3-6. (A): Stress-strain curves of monoliths determined by compression test (parallel to BC layers) with a compression speed of 1 mm/min. (B): Photo images of monoliths after compression test [(a): BC/PLLA100, (b): PLLA100].

Moreover, BC/PLLA showed considerable improvement in terms of brittleness, whereas PLLA100 was cracked and collapsed under 30% strain during compression (the test was continuously conducted after 30% strain as a matter of convenience) (Figure 3-6B). This may be because the 3-D BC network acted as a reinforcement agent, like a steel frame, for the brittle PLLA monoliths.[12] In addition, the mechanical anisotropy of BC/PLLA was observed by the direction of compression (Table 3-2). It was revealed that higher stress was required for the compression parallel to the BC layer than that for the perpendicular. This phenomenon was reported previously, namely, the mechanical strength of BC gel changed dramatically because of its anisotropic structure.[10,11] In this study, the difference between these orientations was limited to within a small range probably because the PLLA unit was filled throughout the BC structure. Thus, it was revealed that the interpenetration of BC fiber efficiently enhanced brittle PLLA monoliths consisting of leaf-like crystals.

Finally, the change in wettability was investigated through a static water angle experiment (Figure 3-7, Table 3-2). The BC/PLLA100 monolith exhibited a notably lower contact angle ($102.1^{o} \pm 1.7^{o}$) than did pristine PLLA ($128.8^{o} \pm 1.1^{o}$) (Figure 3-7A). Furthermore, the BC/PLLA100 monolith spontaneously absorbed water droplets, whereas PLLA100 retained the drops on its surface (Figure 3-7B). Regarding BC/PLLA50 and BC/PLLA75, the hydrophilicity dramatically improved, as water droplets were rapidly absorbed in the monoliths (Table 3-2) and the contact angle was not available. This fact suggests that incorporating hydrophilic BC enables PLLA monoliths to manipulate its wettability. In previous studies, the hydrophilicity of PLLA monoliths was improved using BCNWs. However, the water contact angle remained at 57^{o} in the BCNW/PLLA monolith[14]

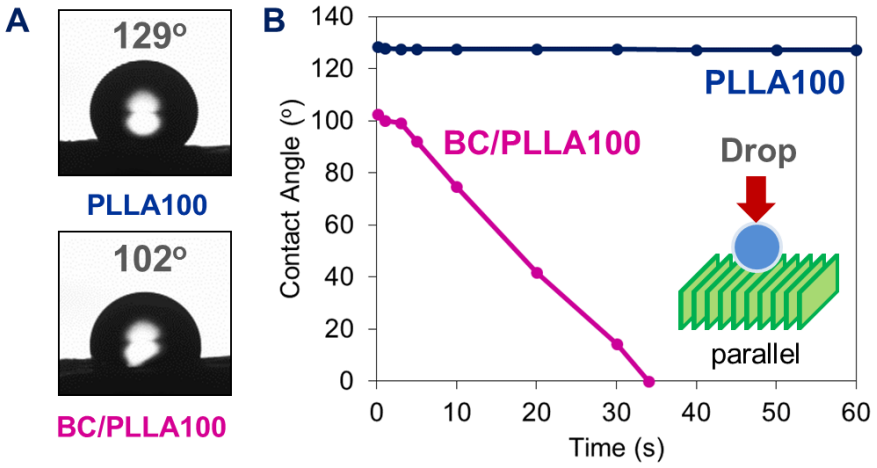

Figure 3-7. (A): Static water contact angle measured on monoliths at 0.1 s after drop parallel to BC layers. (B): Change in absorbability of water droplet between PLLA100 and BC/PLLA100.

In this research, it was demonstrated that a large amount of BC structure can be introduced throughout PLLA monoliths by TIPS technique. In addition, it was found that the hydrophilicity of PLLA monoliths could be easily controlled by the ratio of BC gel (4.4-8.6 wt%).

3.4 Conclusion

In this chapter, the author developed a novel monolithic composite composed of PLLA and BC gel through simple TIPS technology and elucidated the changes in morphology, mechanical properties, and wettability. BC/PLLA monoliths exhibited a unique ivy-like double network wherein a leaf-like PLLA unit and BC fiber were co-existed. It was clearly observed that this ivy-like structure contributed to the reinforcement of PLLA monoliths, and exhibited four times higher compressive strength than that of neat PLLA. Furthermore, it was revealed that the interpenetration of BC structure changes hydrophobic PLLA monoliths to hydrophilic materials and can thus considerably expand the use of PLLA monoliths. Thus, it was demonstrated for the first

time that hydrophilic PLLA monoliths with both high mechanical properties and the ability to control morphology can be prepared by incorporating BC gel and by using a simple TIPS technique.

3.5 References

1. Ghalia, M. A.; Dahman, Y. *J. Polym. Res*. **2017**, 24, 74.
2. Tanaka, T.; Nishimoto, T.; Tsukamoto, K.; Yoshida, M.; Kouya, T.; Taniguchi, M.; Lloyd, D. R. *J. Membr. Sci*. **2012**, 396, 101-109.
3. Tanaka, T.; Tsuchiya, T.; Takahashi, H.; Taniguchi, M.; Ohara, H.; Lloyd, D. R. *J. Chem. Eng. Jpn.* **2006**, 39, 144-153.
4. Jeong, S. I.; Kyoung, E.; Yum, J.; Jung, C. H.; Lee, Y. M.; Shin, H. *Macromol. Biosci.* **2008**, 8, 328-344.
5. Rezabeigi, E.; Wood-Adams, P. M.; Drew, R. A. L. *Polymer* **2014**, 55, 6743-6753.
6. Huang, Y.; Zhu, C.; Yang, J. Nie, Y.; Chen, C.; Sun, D. *Cellulose* **2014**, 21, 1-30.
7. Moon, R. J.; Martini, A.; Nairn, J.; Simonsen, J.; Youngblood, J. *Chem. Soc. Rev.* **2011**, 40, 3941-3994.
8. Shah, N.; Ul-Islam, M.; Khattak, W. A.; Park, J. K. *Carbohydr. Polym.* **2013**, 98, 1585-1598.
9. Czaja, W. K.; Young, D. J.; Kawecki, M.; Brown, R. M. Jr. *Biomacromolecules* **2007**, 8, 1-12.
10. Nakayama, A.; Kakugo, A.; Gong, J. P.; Osada, Y.; Takai, M.; Erata, T.; Kawano, S. *Adv, Funct, Mater.* **2004**, 14, 1124-1128.
11. Haque, M.; Kamita, G.; Kurokawa, T.; Tsujii, K.; Gong, J. P. *Adv. Mater*. **2010**, 22, 5110-5114.
12. Quero, F.; Nogi, M.; Yano, H.; Abdulsalami, K.; Holmes, A. M.; Sakakini, B. H.; Eichhorn, S. J. *ACS Appl. Mater. Interfaces* **2010**, 2, 321-330.
13. Shi, Z.; Zang, S; Jiang, F.; Huang, L.; Lu, D.; Ma, Y.; Yang, G. *RSC Adv.* **2012**, 2, 1040-1046.

14. Luo, H.; Xiong, G.; Li, Q.; Ma, C.; Zhu, Y.; Guo, R.; Wan, Y. *Fiber. Polym.* **2014**, 15, 2591-2596.
15. Martínez-Sanz, M.; Lopez-Rubio, A.; Lagaron, J. M. *Biomacromolecules* **2012**, 13, 3887-3899.
16. Önder, Ö. C.; Yilgöl, E.; Yilgöl, I. *Polymer* **2016**, 107, 240-248.
17. Lloyd, D. R. Kim, S. S.; Kinzer, K. E. *J. Membr. Sci.* **1991**, 64, 1-11.
18. Lloyd, D. R.; Kinzer, K. E.; Tsung, H. S. *J. Membr. Sci.* **1990**, 52, 239-261.
19. Fischer, E. W.; Sterzel, H. J.; Wegner, G. *Kolloid. -Z. Z. Polym*. **1973**, 251, 980-990.
20. Rezabeigi, E.; Drew, R. A. L.; Wood-Adams, P. M. *Ind. Eng. Chem. Res.* DOI: 10.1021/acs.iecr.7b02786.
21. Rezabeigi, E.; Wood-Adams, P. M.; Drew, R. A. L. *J. Polym. Sci. B Polym. Phys*. **2017**, 55, 1055-1062.
22. Pei, A.; Zhou, Q.; Berglund, L. A. *Compos. Sci. Technol.* **2010**, 70, 815-821.
23. Martin, L.; Ossó, J. O.; Ricart, S.; Roig, A.; García, O.; Sastre, R. *J. Mater. Chem.* **2008**, 18, 207-213.
24. Sai, H.; Xing, L.; Xiang, J.; Cui, L.; Jiao, J.; Zhao, C.; Li, Z.; Li., F. *J. Mater. Chem. A* **2013**, 1, 7963-7970.

Concluding remarks

In this doctoral thesis, functionalized PLA monoliths were fabricated through novel TIPS method. PLLA monoliths were blended with enantiometric PDLA or BC gel to improve physical properties through TIPS with ternary solvent, elucidating relationships between structures and characteristics

In Chapter 1, PLLA monoliths with micron to nano scale of frameworks and leaf-like morphology were successfully produced *via* TIPS with ternary solvent using 1,4-dioxane as a good solvent, water as a non-solvent, and 2-butanone as a mid-solvent which controls phase separation. The addition of mid-solvent significantly affects the morphology and crystallization of PLLA, which leads to a precise controllability in morphology and high porosity. A ternary phase diagram of the solvents was proposed for the TIPS, which successfully explained the present results. It was demonstrated that the newly developed, amazingly simple TIPS is ideal for the synthesis of PLLA monoliths compared to the most commonly used TIPS with binary solvent.

In Chapter 2, PLA monoliths containing stereocomplex crystals were successfully produced using enatiometric PLLA and PDLA *via* TIPS developed in Chapter 1. The basic structure of the monoliths was changed drastically from needle-like to spherical morphology until reaching the PLLA/PDLA ratio to equivalence. The PLA monolith prepared from stoichiometric amount of PLLA/PDLA had high sc-crystallinity without any homo-chiral crystals, and it showed higher melting temperature (226 ^{o}C), surface area (131 m^2/g), and water contact angle (144.5^{o}) compared with those of neat PLLA (180 ^{o}C, 86 m^2/g, and 137.5^{o}, respectively). Moreover, this sc-PLA monolith exhibited excellent resistance to good solvents of PLLA, whereas the pristine PLLA monolith was dissolved instantly in these solvents.

In Chapter 3, PLLA monoliths were successfully blended with BC gel *via* TIPS developed in Chapter 1 and freeze drying technique. BC/PLLA composite monoliths exhibited unique ivy-like structure composed of leaf-like PLLA units and BC fiber network. The interpenetrating BC fiber allowed PLLA monoliths to have four times higher compressive strength than the pristine PLLA. Moreover, hydrophilicity of the PLLA monoliths was easily controlled by the incorporation of BC. Neat PLLA monoliths showed high static water contact angle up to $128.8^{o} \pm 1.1^{o}$, while BC/PLLA monoliths exhibited much lower contact angle ($102.1^{o} \pm 1.7^{o}$) and great absorbability to water.

In conclusion, functionalized PLA monoliths were successfully tailored through TIPS using the ternary solvent (1,4-dioxane/2-butanone/water) blending with soluble or insoluble polymers. The fabricated monoliths with unique 3D morphology exhibited reinforced properties such as high heat resistance, chemical resistance, mechanical strength, and hydrophilicity, which can be valuable for practical use. The technique developed in this thesis extends the scope of the usage of PLA monoliths and gives great impact on the development in a number of fields such as medical, filtration technology, and material design as the concept to produce next-generation porous material. The author believes the technology marked here will open the application of PLA monoliths and contribute to the sustainable society.

List of publication

1. Unique leafy morphology of poly(lactic acid) monoliths controlled *via* novel phase separation technology

   Tomonari Kanno, Hiroshi Uyama

   RSC Advances **2017**, 7, 33726-33732.

2. Unique transitions in morphology and characteristics of porous poly(lactic acid) enantiomers

   Tomonari Kanno, Hiroshi Uyama

   Macromolecular Chemistry and Physics **2018**, DOI: 10.1002/macp.201700547.

3. Unique ivy-like morphology composed of poly(lactic acid) and bacterial cellulose cryogel

   Tomonari Kanno, Hiroshi Uyama

   ACS Omega, **2018**, 3, 631-635.

Acknowledgements

This study was completed from 2015 to 2018 at the Department of Applied Chemistry, Graduate School of Engineering, Osaka University.

First and foremost, I would like to thank my supervisor, Prof. Hiroshi Uyama, for his helpful and constructive supervision, constant guidance, and invaluable discussion. Without his encouragement, this dissertation would not have materialized. He is not only an excellent professor but also a symbol in many aspects of my life in Osaka. I also sincerely thank him for providing me with a great deal of chance to acquire new and different experience. The precious experience that I have absorbed here will guide my future career.

I am profoundly grateful to Assistant Prof. Takashi Tsujimoto. He gave insightful comments and suggestions to every challenge I have faced throughout this study. Without his wisdom, this thesis would not have been possible.

Special thanks also to Associated Prof. Taka-aki Asoh and Assistant Prof. Urara Hasegawa for their kind help and expert advises.

I would like to express my gratitude to Prof. Takashi Hayashi and Prof. Masaya Nogi for their valuable and constructive comments on preparation of this thesis.

My heartfelt appreciation goes to Prof. Tsuyoshi Inoue and Associate Prof. Eiichi Mizohata for their encouragement and helpful advises during my life in doctoral course. And I also give my sincere thanks to Dr. Yasushi Takeuchi and Dr. André J van der Vlies for invaluable suggestions and supports.

I owe my deepest gratitude to Prof. Hideko T. Oyama. Department of Chemistry, Rikkyo University, for her continuous encouragement and support to pursue my doctoral degree.

My appreciation goes also to the previous and current fellow in the lab: Dr. Nao Hosoda, Dr. Guowei Wang, Dr. Boxing Zhang, Dr. Tengjao Wang, Dr. Hyunhee Shim, Dr. Yu Shu, Mr. Qidong Wang, Ms. Zhaohang Yang, Mr. Masatoshi Kato, Mr. Yuki Tsutsumi, Ms. Ayumi Dobashi, Ms. Manami Morisaki, Mr. Tomoki Kasahara, Mr. Kyeong Yeol Kim, Mr. Keng Yao Tang, Mr. Jia Yu Chen, Mr. Naharullah Bin Jamaluddin, Mr. Toshiki Tamiya, Mr. Yuki Hayashi, Mr. Yusuke Hinamoto, Mr. Hayate Hirono, Mr. Shunsuke Mizuno, Mr. Masahiro Namba, Mr. Jiaji Yang, Ms. Moe Sugahara, Mr. Ginga Hoshi etc. for their kind help, assistance, and friendship. And I also appreciate the warm-hearted support from Ms. Yoko Uenishi, Ms. Tomoko Shimizu, Ms. Kyoko Tanimura, Ms. Chiaki Yoshizawa, Ms. Akiko Nakano, and Ms. Mie Iwamoto.

I am also grateful to the Japan Society for the Promotion of Science (JSPS) for providing a doctoral fellowship. This study is financially supported by a Grant-in-Aid for Scientific Research from JSPS (Grant Number 17J01410)

Finally, I would like to extend my appreciation to my family for their endless love, support, and understanding.

Janualy 2018

Tomonari Kanno